Relationship of N-glycans to Neuronal Dysfunction

By

Austin Whitman

July 2019

Director of Thesis: Dr. Ruth Schwalbe

Major Department: Biochemistry

N-glycosylation is important in regulating protein activity and serves several vital roles contributing to protein folding, protein assembly, stability, and interactions. Changes in branching of N-glycans are linked to development and maintenance of multicellular organisms. All N-glycans share a common core sugar sequence and are classified as three major types: oligomannose, complex, and hybrid. Here the aim is to determine the roles N-glycans have in cell behavior, as well as, vertebrae development. To characterize the contribution of complex N-glycans to neuroblastoma (NB), CRISPR-Cas9 technology was employed to silence the *Mgat2* gene in a NB cell line. *Mgat2* encodes for GlcNAcT-II, N-acetylglucosaminyltransferase-II, responsible for converting hybrid type N-glycans to complex type. Lectin binding studies were conducted to support the successful knockout of *Mgat2.* Electrophoretic mobility shifts of Kv3.1, a voltage-gated K^+ channel, supports that N220 and N229, possess complex N-glycans in our wild type cell line and hybrid N-glycans in our N-glycosylation mutant cell line. Wound healing, anchorage-independent growth, and MMP-2 expression studies found that the loss of *Mgat2* resulted in decreased tumorigenicity. *Mgat1b* was silenced in zebrafish to study how increased oligomannose N-glycans affect vertebrae

development. *Magt1b* encodes for GlcNAct-I, responsible for converting oligomannose N-glycans to hybrid type, which in turn form complex N-glycans. DNA sequencing and various genotyping of zebrafish generations support the knockout of *Mgat1b.* The loss of *Mgat1b* resulted in decreased embryo viability but also increased the number of eggs spawned. Overall, this data reveals that complex N-glycans contribute to an increase in NB tumorigenicity, and also, increased levels of oligomannose N-glycans impede development of embryos in vertebrae.

Relationship of N-glycans to Neuronal Dysfunction

A Thesis

Presented to the Faculty of the Department of Biochemistry

Brody School of Medicine

East Carolina University

In Partial Fulfillment of the Requirements for the Degree

Master of Science in Biomedical Sciences

By

Austin A. Whitman

July 2019

Relationship of N-glycans to Neuronal Dysfunction

By

Austin Whitman

APPROVED BY:

DIRECTOR OF THESIS: _____
Dr. Ruth A. Schwalbe, PhD

COMMITTEE MEMBER: _____
Dr. Yan-Hua Chen, PhD

COMMITTEE MEMBER: _____
Dr. Brian Shewchuk, PhD

COMMITTEE MEMBER: _____
Dr. Douglas Weidner, PhD

CHAIR OF DEPARTMENT: _____
Department of Biochemistry:
Dr. Richard Franklin, PhD

DEAN OF THE
GRADUATE SCHOOL: _____
Paul J. Gemperline, PhD

Dedication

I would like to thank my friends, family, and loved ones for their moral support.

Especially my Mother and Father, thank you all so much.

Acknowledgements

I graciously acknowledge my research advisor, Dr. Ruth Schwalbe, for her guidance, knowledge, and advice throughout my studies. As well as our lab technician, Kristen Hall, for her assistance, guidance, and knowledge. I wish to acknowledge that the novel cell line was designed and engineered by Ms. Hall and Dr. Schwalbe. I acknowledge Dr. Weidner for his assistance in flow cytometry. I offer my appreciation to Kristen Hall, and Drs. Weidner and Schwalbe for guiding me through experimental protocols, data analysis, and the contribution of results to my thesis. I would also like to thank Cody Hatchett for his assistance during the Zebrafish embryo studies.

I would also like to recognize my committee members; Dr. Chen, Dr. Shewchuk, Dr. Schwalbe, and Dr. Weidner for their insight into my project. I acknowledge the faculty and staff of the Departments of Biochemistry and Molecular Biology at East Carolina University for allowing me to participate this Master's program.

Table of Contents

List of Figures

List of Abbreviations

AD	Alzheimer's Disease
APP	Amyloid Precursor Protein
APS	Ammonium Persulfate
Aβ	β-amyloid
CDG	Congenital Disorders of Glycosylation
CRISPR	Clustered Regularly Interspaced Short Palindromic Repeat
crRNA	CRISPR RNA
DMEM	Dulbecco's Modified Eagle Media
DNA	Deoxyribonucleic Acid
ECM	Extracellular Matrix
EDTA	Ethylenediaminetetraacetic Acid
EGFP	Green Fluorescent Protein
Endo H	Endoglycosidase H
E-PHA	*Phaseolus vulgaris* Erythoagglutinin
ER	Endoplasmic Reticulum
FBS	Fetal Bovine Serum
GlcNAcT	N-acetylglucosaminyltransferase

GNL	*Galanthus nivalis* lectin
GnT-II	GlcNAcT-II
Golgi	Golgi Apparatus
gRNA	Guide RNA
HuNB	BE(2)C Human Cell Line
HuNB(+/-*Mgat2*)	Rescued N-glycosylation Mutant Human Neuroblastoma Cell Line
HuNB(-*Mgat2*)	BE(2)C Engineered Human N-glycosylation Mutant
Kv	Voltage-gated Potassium Channels
L-PHA	*Phaseolus vulgaris* Leucoagglutinin
MMPs	Matrix Metalloproteases
NB	B35 Rat Cell Line
NB(-*Mgat2*)	B35 Engineered Rat N-glycosylation Mutant
PAM	Protospacer Adjacent Motif
PBS	Phosphate Buffered Saline
PCR	Polymerase Chain Reaction
PNGase F	Peptide N-glycosidase F
PVDF	Polyvinylidene Difluoride
RIPA	Radioimmunoprecipitation Assay Buffer

RNA	Ribonucleic Acid
SDS	Sodium Dodecyl Sulfate
SDS-PAGE	Sodium Dodecyl Sulfate Polyacrylamide Gel Electrophoresis
TEMED	Tetramethylethylenediamine
TIMPs	Tissue Inhibitor of Metalloproteases

Introduction

N-glycans are oligosaccharides that are a component of glycoproteins. These glycans are attached to a nitrogen atom of asparagine side chains of proteins. Asparagine is the first amino acid residue of a tripeptide N-glycosylation site. The attachment of these glycans are done, co- and post-translationally, through a process called N-glycosylation (Stanley, Taniguchi, and Aebi 2017). There are three major types of N-glycans: oligomannose, hybrid, and complex. The enzymes known as N-acetylglucosaminyltransferases or GlcNAcTs are responsible for initiating the branch points on a common core sugar sequence, which creates the three different types of glycans. These GlcNacTs are encoded by eight *Mgat* genes (Stanley 2009). The glycosylation of proteins is very important in the realms of multicellular organisms because most of membrane proteins are N-glycosylated (Hall et al. 2013; Hall et al. 2014). N-glycosylation is important in regulating protein activity and serve several vital roles contributing to protein folding, protein assembly, stability, and interactions, such as E-cadherin (Helenius and Aebi 2004; Vaki and Lowe 2009;Hall et al. 2013; Hall et al. 2015). N-glycans are involved in cellular recognition events that can give rise to cancerous properties (Hall et al. 2015; Hall et al. 2018). These cancerous properties include: cell signaling, cell migration, cell invasion, cell proliferation, and cell-cell adhesion (Hall et al. 2016; Hall et al. 2018). N-glycans have also been found to contribute to the spatial localization of voltage gated potassium Kv3.1 channels (Hall et al. 2015), a critical neuronal potassium channel, and E-cadherin (Hall et al. 2013; Hall et al. 2014), a transmembrane protein involved in cell to cell adhesion in the plasma membrane.

N-glycosylation is a process found throughout all aspects of life. Although there are differences among N-glycosylation pathways there are three processes that are the basis for N-glycosylation (Schwarz and Aebi 2011). The first being the synthesis of the glycan on a lipid anchor through glycosyltransferases by incorporating monosaccharides in a stepwise process. This oligosaccharide then reorients from the cytosolic to the luminal side of the of the endoplasmic reticulum (ER) or plasma membrane. This oligosaccharide will serve as a donor for glycosylation of a protein. The second process is the translocation of proteins to the ER to be the acceptor of the glycan. The third process is the attachment of the glycan to the proteins with a consensus sequence of N-X-S/T, where X is any amino acid beside proline (Schwarz and Aebi 2011). This is done by an oligosaccharyltransferase, which transfers the oligosaccharide to the asparagine of the consensus sequence (Helenius and Aebi 2004; Schwarz and Aebi 2011). In eukaryotes, once the N-glycan becomes linked to the protein it is then able to be modified. Processing in the Golgi allows for species specific or cell type specific types of N-glycans (Schwarz and Aebi 2011). The common core sequence of all N-glycans found in all eukaryotes is, Manα1-3(Manα1-6)Manβ1-4GlcNAcβ1–4GlcNAcβ1–N-X-S/T (Stanley, Taniguchi, and Aebi 2017). As mentioned previously, N-glycans are classified into three major types. Oligomannose type N-glycans possess only mannose residues extending from the common core. Hybrid type have mannose residues attached to the Manα1-6 arm and a GlcNAc residue attached to the Manα1-3 arm. Complex type have at least one GlcNAc residue attached to Manα1-3 arms (Stanley, Taniguchi, and Aebi 2017).

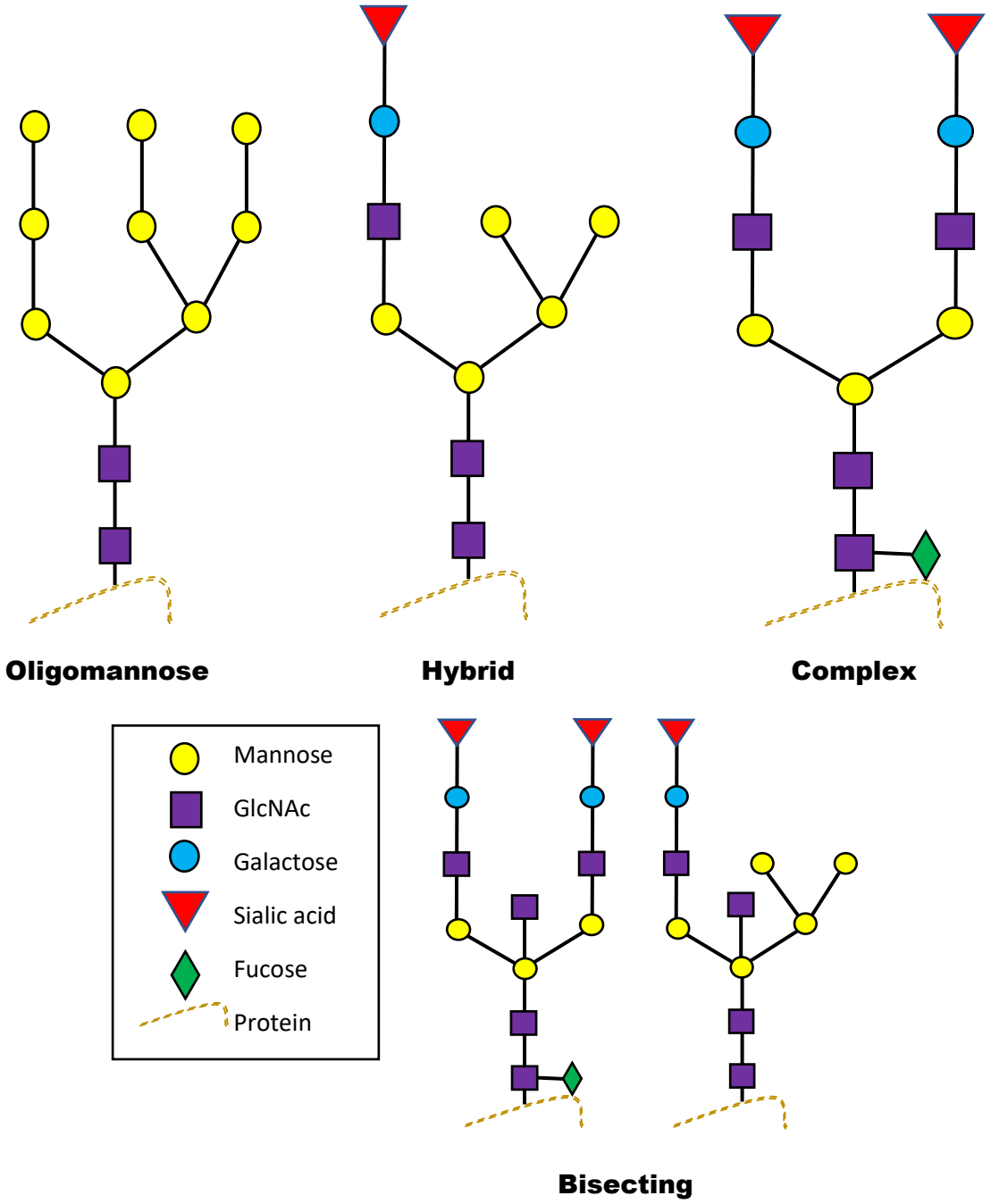

Figure 1. Types of Common N-Glycans. The major three types of N-glycans; oligomannose, complex, and hybrid, as well as bisecting type. They key denotes the monosaccharide residues of each oligo/polysaccharide.

Congenital disorders of glycosylation (CDG) are genetic diseases caused by deficiencies in the glycosylation of glycoconjugates, such as glycoproteins and glycolipids (Jaeken 2010). It is thought that the CDGs that are related to proteins are due to deficiencies in the N-glycosylation pathway (Scott et al 2014). The N-glycosylation process has three cellular components: cytosol, ER, and the Golgi (Jaeken and Heuvel 2014). It begins in the cytosol, where fructose 6-phosphate is converted to GDP-mannose, a mannose donor. In the lumen of the ER, the dolichol-linked oligosaccharide $GlcNAc_2Glc_3$ is built and transported from dolichol to the asparagines of newly formed proteins (Jaeken and Heuvel 2014). This glycan then has a mannose and three glucoses removed before going to the Golgi. While in the Golgi, five more mannoses are removed and replaced with two N-acetylglucosamine residues, galactose and sialic acid. The most common N-glycosylation disorders were found to be those with a cytosolic assembly defect (Jaeken and Heuvel 2014). These patients suffer from mild to severe neurological disease. The second most common form of N-glycosylation disorder is an ER assembly defect (Jaeken and Heuvel 2014). The majority of CDG patients have a neurological disease affecting multiple systems, such as the central nervous system, cellular transport, muscle function, immunity, hormones, coagulation, and regulatory processes. The number of CDGs caused by N-glycosylation defects are still on the rise. Around 50 clinical syndromes have been found to be the result of defects in N-linked glycosylation (Scott et al 2014). CDGs emphasizes the role N-glycans have on the growth and development of neural tissue.

Voltage-gated potassium (Kv) channels are found throughout the central nervous system and play a crucial role in regulating action potentials of neurons (Hall et al.

2011). The Kv superfamily consists of more than 140 members, being one of the largest groups of signal transduction proteins (Frank et al. 2005). Kv channels have been found to be tetramers of four identical subunits structured into a ring, making up the wall of the trans-membrane K^+ pore. Each subunit consists of six hydrophobic α-helical transmembrane segments (S1-S6) spanning the membrane, S4 acting as a voltage sensor (Yellen 2002). The S4 helix possess multiple positively charged residues that respond to the changes in membrane voltage (Rodriguez-Menchaca et al. 2012). When the opening of the Kv channel is initiated, a conformational change in the voltage-sensor domains results in a transfer of charges across the membrane. Charged residues of the voltage-sensor domains move across the transmembrane field and contribute to the gating charge (Lee et al. 2005). At depolarization, the transition of these residues from a resting state to an activated state and then a joint conformational change leads to the opening of the pore (Rodriquez-Menchaca et al. 2012). Kv channels are selective for K^+ over other cations, such as Na^+, even though it's much smaller. This is due to water-K^+ interactions being disrupted and replaced by interactions with carbonyl groups of the channel protein (Gutman et al. 2005). The Kv channels have fast activation and deactivation rates and are activated at more depolarized potentials compared to other channels (Rudy and McBain 2001). Kv channels are also known to have non-conducting properties, such as cell migration, cell proliferation, and cell-cell interaction (Kaczmarek 2006; Hall et al. 2011:2017).

The Kv3.1 channel have been found to possess two highly conserved glycosylation sites, N220 and N229, at the S1-S2 linker (Shi and Trimmer 1999; Brooks, Corey, and Schwalbe 2006). Recent studies have shown that the vacancy of these

glycosylation sites in Kv3.1, an unglycosylated Kv channel, as well as partially glycosylated Kv3.1 result in slower activation and deactivation rates of the channel when compared to a fully glycosylated Kv3.1 within rat neuroblastoma derived cells. The migration of these neurons also slowed as the glycosylation sites became more vacant (Hall et al. 2011). More recent studies have shown, that the substitution of complex type N-glycans for hybrid type N-glycans attached to Kv3.1 channels affected the localization of the channel as well as the opening and closing rates (Hall et al. 2015; Hall et al. 2017). Kv3.1 with complex type N-glycans localized to neurites more so than Kv3.1 with hybrid type, which localized more in the cell body. The opening and closing rates of the Kv3.1 channels were slower in cells predominately expressing hybrid type N-glycans in comparison to cells predominately expressing complex type (Hall et al. 2017). The Kv3.1 channel has also been shown to contribute to the regulation of oligodendrocyte progenitor cell development and axon myelination (Tiwari-Woodruff et al. 2006). These results are indicative that the glycosylation of the Kv3.1 glycoprotein plays a crucial role in the conducting and non-conducting properties of the channel. The disruption of the N220 and N229 glycosylation sites in Kv3.1, as well as different types of glycans, alter channel function, and this is likely to occur in patients diagnosed with CDGs (Hall et al. 2011; Brooks, Corey, and Schwalbe 2006; Hall et al. 2017). The dysfunction and expression levels of Kv3 channels have also been associated with diseases of the nervous system and cancer (Waters et al. 2006).

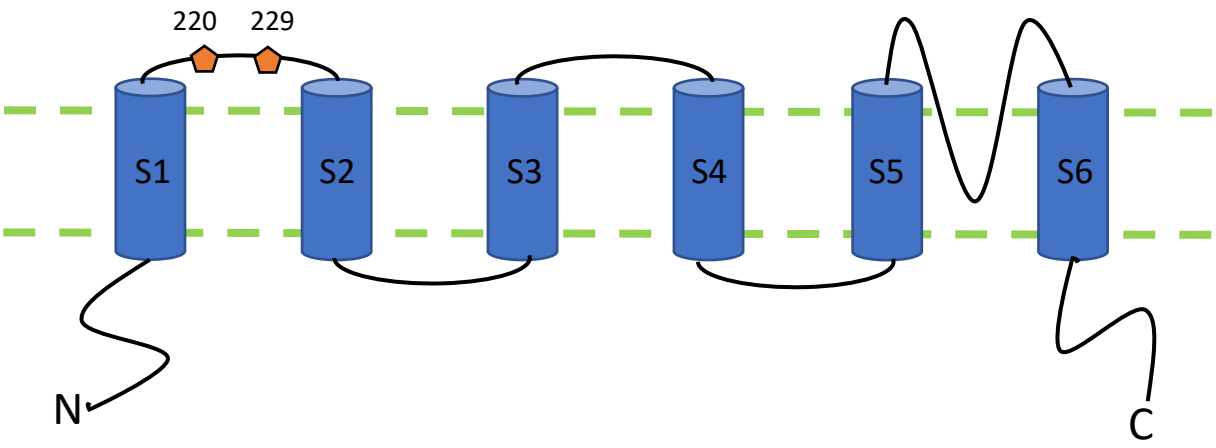

Figure 2. Kv3.1 Model. Topological structure of Kv3.1 channel. Cylinders represent alpha-helices. Orange pentagons represent the two conserved glycosylation sites at N220 and N229 located outside the cell. Dashed green lines represent the cell membrane. N-terminus and C-terminus are localized in the cytosol, attached to the S1 and S6 α-helixes, respectively.

In 2018, the estimated number of new cancer cases exceeded 18 million, with more than 9 million cancer related deaths (Bray et al. 2018). With increasing life expectancy and birth rate, the cancer incidence and mortality are continuing to grow (Omaran 1971; Gersten and Wilmoth 2002). It is estimated that the Americas will account for 21% of cancer incidence and 14.4% of mortality worldwide. The most commonly diagnosed and leading cause of cancer death is lung cancer, followed by female breast cancer (Bray et al. 2018). Cancer is a disease, or group of diseases, where abnormal cellular growth gives cells the potential to spread or invade throughout other parts of the body, through a process called metastasis (World Health Organization 2018; National Cancer Institute 2007). Cancer cells that lack the ability to invade or metastasize into neighboring tissue grow into benign tumors, which can grow into large masses, but can be easily removed depending on location (National Cancer Institute 2007). Most cancers are caused by genetic mutations from environmental and lifestyle factors, including age, diet, and exercise. Around 5-10% of cancer cases are hereditary (Anand et al. 2008). For a cell to transform into a cancer cell, the genes that regulate cell differentiation and growth must be disrupted (Croce 2008). Two categories of these genes are oncogenes and tumor suppressor genes, which promotes cell growth and proliferation and the other inhibits cell growth and division, respectively (Knudson 2001).

During cancer development, cancer cells interact with the surrounding extracellular matrix (ECM), surrounding cells, growth factors, and cytokines affiliated with the ECM (Kessenbrock, Plaks, and Werb 2010; Murphy 2008). Hallmarks of cancer include proliferation, migration and invasion, metastasis, and angiogenesis that are affected by the surrounding cell environment. Crucial molecules throughout these

processes are matrix metalloproteases (MMPs) since they degrade cell adhesion molecules, influencing cell-cell and cell-ECM interactions (Gialeli, Theocharis, & Karamanos 2011). MMPs are potential diagnostic and prognostic biomarkers in cancer development and have been considered for therapeutic targets because of their ability to degrade the basement membrane (Roy, Yang, and Moses 2009). Their proteolytic activity allows for cell invasion, metastasis, and angiogenesis. MMPs increase the availability of growth factors and cytokines, by cleaving precursor molecules into their active forms (Murphy 2008). The release of various growth factors and cytokines contribute to tumor cell proliferation (Loechel et al. 2000). MMPs degrade E-cadherin and integrin allowing for cells to detach from the ECM and surrounding cells, increasing cellular migration (Murphy 2008). Different members of the MMP family have been shown to exert different roles at different stages of cancer development. MMP-8 has been shown to inhibit metastasis in certain cancers by preserving tumors, while MMP-2 and MMP-9 are known to degrade the ECM, promote cell proliferation, and upregulate angiogenesis (Decock et al. 2008).

MMPs are modified co- and post-translationally through the process of glycosylation where either N- or O-glycans can be attached to the protein (Rudd and Dwek 1997). The catalytic sites of MMPs are not O-linked glycosylated, but instead have conserved N-linked glycosylation sites for potential glycosylation (Boon et al. 2016). The conservation of these N-glycosylation sites supports that N-glycans may play an important biological function in MMP regulation and function (Rudd and Dwek 1997). Regulators and substrates of MMPs are also glycosylated. Changes in the glycosylation status of these molecules may have an impact, either directly or indirectly,

on MMP function. Tissue inhibitor of metalloproteinases (TIMPs) are important regulators of MMPs, inhibiting their proteolytic activity (Murphy et al. 1991). TIMP-1 and TIMP-3 are known to contain N-linked glycans (Sutton, O'Neil, and Cottrell 1994). Altered glycosylation of TIMP-1 and TIMP-3 have a direct effect on MMP-2 and MMP-9 activity by interfering with their interaction (Boon et al. 2016). Glycosylation of MMP substrates have been found to affect their association with MMPs, determining the cleavage sites of some substrates like collagen, which is extensively glycosylated (Ranjan and Kalraiya 2014; Van den Steen 2002). Much remains to be discovered about glycosylation effects on MMP activity, due to the heterogeneity of the attached glycan structures increasing the diversity MMP structures and functions. This diversity adds difficulty to the analysis of MMPs (Boon et al. 2016).

Neuroblastoma is a cancer that is derived from the sympathetic nervous system (Ho et al. 2016). The cell of origin is believed to be an incompletely committed precursor cell from neural-crest tissues. Neuroblastoma is the most common solid tumor found in children, with the median age of diagnosis being 17 months, and is responsible for 15% of cancer related deaths in children (Maris 2010; Ho et al. 2016). The overall prognosis of neuroblastoma patients has improved with therapeutic advances, but long-term survival of aggressive forms of neuroblastoma remains poor even with advanced intensive therapy (Ho et al. 2016). 50 to 60% of patients with more aggressive forms have a relapse and there are no treatment regimens known to be a curative. Although, recent methods have been developed to help prolong survival (Maris 2010). Like other types of cancer, the alteration of cell surface glycans have been a characteristic of tumor development and progression (Hall et al. 2018; Fuster and Jeffrey 2005). It has

been found that glycans regulate the proliferation, invasion, and metastasis of tumors (Fuster and Jeffrey 2005). Although, the types of N-glycans and their roles in cancer development are still being determined (Ho et al. 2016).

N-glycans can be found attached to the extracellular regions of various types of membrane proteins, contributing to their architecture and therefore their function, which affects cellular properties (Hall et al. 2016). Alterations in the presence and type of N-glycans on transmembrane proteins have been shown to change the spatial arrangement of E-cadherin molecules (Hall et al. 2014) and Kv channels (Hall et al. 2013; Hall et al. 2017). The usefulness of N-glycan based therapeutics in cancer treatment was found in metastatic cancers (Goee et al. 1994; Shaheen et al. 2005). Swainsonine, an indolizidine alkaloid, inhibits the activity of Golgi mannosidase II, altering the N-glycosylation pathway by preventing the processing of hybrid type N-glycans to complex type (Tulsiani and Touster 1983). Phase 1 and 1B clinical trials of swainsonine have shown to be effective in treating multiple types of human cancers (Goss et al. 1994), but phase 2 trials have found it to be ineffective in patients with advanced renal carcinoma (Shaheen et al. 2005). Studies have also shown that increased levels of bisecting N-glycans suppressed lung cancer metastasis (Yoshimura 1995). Bisecting N-glycans have also been shown to strengthen the role of E-cadherin and increase the stability of adherens junctions, which plays a key role in the suppression of tumor development (Yoshimura 1996). Complex N-glycans, catalyzed by GNT-V, with β1,6 N-acetylglucosamine were shown to weaken E-cadherin mediated cell-cell adhesion promoting tumor progression (Pinho et al. 2013). Oligomannose type

N-glycans were also shown to have a greater impact on strengthening adherens junctions compared to complex type (Liwosz et al. 2016).

N-glycans are considered to be involved in Alzheimer's disease (AD) onset and progression. However, there have only been a few studies focusing on the glycobiology in AD (Schedin-Weiss, Winblad, and Tjernberg 2014). Alzheimer's disease, the most common cause of dementia, leads to memory loss and a decline in cognitive abilities. Alzheimer's worsens over time and as it progresses memory loss becomes more severe and the ability to respond to one's environment may be lost (Armstrong 2013). The greatest risk factor is aging, and the majority of people with AD are above the age of 65. A prevalent structure found throughout the brain of Alzheimer's victims, known to damage nerve cells, is β-amyloid (Aβ) (Armstrong 2013). An increase in Aβ levels has crucial effects in both familial and sporadic cases (Cai, Golde, and Younkin 1993). Aβ is secreted into the spaces between nerve cells, blocking synapses. Cortico-cortical pathways in the brain are severely affected by the release of Aβ (Armstrong 2013). Aβ is created from amyloid precursor protein (APP), which is known to be glycosylated (Cai, Golde, and Younkin 1993; Schedin-Weiss, Winblad, and Tjernberg 2014). Aβ production takes place within the cell and gets processed through the golgi network (Barao et al. 2016). It is then secreted outside the cell, after becoming glycosylated with O- and N-glycans. While the precise role of individual glycans in AD are mostly unknown, recent studies have revealed that glycans have a significant impact by modifying the function of proteins known to affect Aβ synthesis and degradation (Schedin-Weiss, Winblad, and Tjernberg 2014). Further studies on the roles of N-

glycosylation in AD may reveal glycan-based therapeutic targets (Kizuka, Kitazume, and Taniguchi 2017).

Clustered Regularly Interspaced Short Palindromic Repeat, better referred to as CRISPR, has taken the world by storm and is being utilized by thousands in the scientific community. CRISPR originates as an adaptive immune system employed by various microbes to protect themselves against invading viruses (Lander 2016). This adaptive immunity involves three steps: adaption, expression, and interference. During the adaption step, a segment of the invading DNA, the protospacer, is targeted and cleaved by a Cas1-Cas2 protein complex. This fragment of viral DNA, the protospacer, is then incorporated into the CRISPR array. The CRISPR array is a small stretch of DNA composed of alternating repeat sequences separated by target specific protospacers. The protospacers give the microbe an embedded memory for specific viral infections. The Cas1-Cas2 complex binds to the viral DNA by attaching to an adjacent motif to the protospacer sequence, known as the protospacer adjacent motif (PAM). This PAM site allows for self/non-self-recognition since there is a PAM absence in the host microbe's DNA and a PAM presence in the target DNA (Koonin, Makarova, and Zhang 2017; Mougiakos et al. 2016). The expression step is when the CRISPR array is transcribed into pre-crRNA and is then processed into mature crRNA (CRISPR RNA) guides by type dependent proteins. A Cas-crRNA complex (CRISPR ribonucleoprotein) is then formed. During the interference step, the Cas-RNA complex searches the invasive DNA for a PAM site adjacent to nucleic acid targets complementary to the crRNA and then binds. After binding, the target DNA is then

degraded by a Cas nuclease, protecting the host cell (Koonin, Makarova, and Zhang 2017; Matharu et al. 2019).

The CRISPR-Cas systems of adaptive immunity are constantly engaged in an arms race with viruses. This has led to rapid evolution of the *Cas* genes, the diversity found in the gene repertoires and structure of the CRISPR-*Cas* loci. There are two classes of CRISPR-Cas systems, multi-subunit effector complexes in Class 1 and single-protein effector modules in Class 2. Each class is made up of three types, with each type possessing their own subtypes. The two major modules of the CRISPR-Cas systems consist of adaption (protospacer acquisition) and effector functions, the pre-crRNA processing, and the recognition and cleavage of target DNA. The adaption module is the least variable amongst CRISPR-Cas systems, consisting of the highly conserved endonuclease Cas1 and subunit Cas2. The effector modules are highly variable between CRISPR-Cas types and subtypes (Mohanraiu et al. 2016). The Class 1 systems, types I, III, and IV, are found in bacteria and archaea, with several Cas proteins interacting to form effector complexes in an uneven stoichiometry. The rarer Class II systems, predominately found in bacteria, include types II, V, and IV. The class 2 type II effector, Cas9, is well characterized as an RNA-dependent endonuclease containing the nuclease domains, HNH and RuvC. These domains are responsible for the cleaving of the target and displaced strand, respectively. The ability to program sequence specific DNA targeting and cleaving by the Cas9 has allowed CRISPR-Cas to be utilized as tools for genetic engineering and gene regulation. Cas9 has been demonstrated to efficiently create indels (insertions/deletions) at precise locations using gRNA (guide RNA) (Koonin, Makarova, and Zhang 2017).

Zebrafish (*Danio rerio)* possess many attributes making them an ideal model organism for knockout studies looking into vertebrae development and gene function. One of the many advantages to using zebrafish is that its genome has fully been sequenced (Howe et al. 2013). Their fast and short life cycles as well as their large clutch sizes make it easier to conduct genetic studies. Its embryonic development is rapid, and embryos are large and transparent, allowing for easily observable embryonic stages of development (Dahm 2006). Genetic screening has identified many mutant phenotypes which resemble clinical human disorders, providing an approach for the study of various disease states (Dooley and Zon 2000). Zebrafish also have well documented and testable behaviors. Zebrafish are social animals and their social interactions develop into long term and stable dominance relationships (Park et al. 2018). They are also shown to be similar to other mammalian models in toxicity testing, as well as having similar sleep patterns (Jones 2007).

Zebrafish growth and development are dependent upon many environmental factors, such as population density, temperature, water quality, and nutrition (Singleman and Holtzman 2014). Zebrafish offspring are termed embryos until they hatch, which occurs 48-96 hours after fertilization. Once a zebrafish hatches it is then in the larval stage, which lasts around 6 weeks, when the fish nearly triples in length (Parichy et al. 2009). During the larval stage, the fish progresses through a series a morphological changes transforming the fins, pigment pattern, and body systems, such as the nervous system (Parichy et al. 2009; Singleman and Holtzman 2014). The fish then enters into the juvenile stage. At this stage the fish has attained most adult characteristics but are not sexually mature. Juvenile fish have a complete pattern of scales and a complete

loss of the larval fin fold (Parichy et al. 2009). The juvenile stage can occur as early as 4 weeks after fertilization and end up to 12 weeks after fertilization (Singleman and Holtzman 2014). The adult stage is defined by the production of gametes and secondary sexual characteristics (Parichy et al. 2009). These stages are easily visible and identifiable under a microscope, without the need to kill or stain the fish, being another good example of why zebrafish are a widely used model. It has also been found that age has become a less reliable way of measuring maturity and that fish size is used as a better approximation of maturation. Using the standard length of the fish has been accepted as a strategy for defining developmental maturation (Parichy et al. 2009; Singleman and Holtzman 2014).

As a vertebrae model, zebrafish have been used to study the characteristics of neurogenesis. Neurogenesis is the process by which undifferentiated neural progenitor cells mature into functional neurons. During early embryonic development, the formation of the nervous system is initiated by the specification of the neuroectoderm, through a process called neural induction (Schmidt, Strähle, and Scholpp 2013). During this process, multiple signaling factors promotes the cells in the dorsal ectoderm to form the neural plate, a pseudostratified epithelial structure. The neural plate then converges to form the neural keel which then fuses into the neural rod at the dorsal midline. The neural rod inflates to form the neural tube, the hollow structure from which the brain and spinal cord form. Once the lumen of this neural tube is formed an increasing number of cells begin dividing (Schmidt, Strähle, and Scholpp 2013). As the neural progenitor cells continue to divide, the apically derived daughter cells become neurons and the basal daughter cells replenish the apical cells. Notch signaling is responsible for the

proliferation of the basal cells and differentiation of apical cells (Dong et al. 2012). The dividing cells migrate from the apical side of the neural epithelium to the pial side through a process termed interkinetic nuclear migration. Once a cell has migrated to their designated location, then they are able to generate neural circuitry (Baye and Link 2008).

Zebrafish continue to grow as adults. Within their adult brain there are several zones that constantly proliferate during homeostasis and contribute to the continuous growth of the brain. All studied vertebrae have displayed various degrees of adult neurogenesis. Non-mammalian vertebrates have shown to possess more adult neurogenesis than mammals (Kizil et al. 2012). So far, teleost fish, such as zebrafish, exhibit the most adult neurogenesis and have numerous proliferation zones. Most of the progenitor activity has been shown to take place within the telencephalon, among all classes of vertebrae (Kizil et al. 2012). The telencephalon is the largest portion of the forebrain, consisting of the cerebral cortex, hippocampus, amygdala, olfactory bulb, and basal ganglia (Adolf et al. 2006). Zebrafish can offer an opportunity to apply various tools and methods to study the roles N-glycans play in neurogenesis and neuronal function, as well as behavior and motor control.

The behavior of an organism is how it interacts with its environment (Orger and de Polavieja 2017). Neuroscientists have studied behavior to assess the function of the brain. Complex behaviors are often the summation of simpler motor patterns. Breaking down behavior into more discrete aspects can allow the understanding of the neural systems and their organization. Much of the work on zebrafish has been conducted during the early larval stages, when the fish are small and transparent. Common studies

look into reflexive responses, swimming pattern, feeding pattern, aggression, and mating (Orger and de Polavieja 2017).

Two neuroblastoma cell lines were used throughout this thesis, the BE(2)C human neuronal cell line and the B35 rat neuronal cell line. B35 cells were derived from tumors found in the neonatal central nervous system of a rat. These cells are widely used as a model for signaling pathways that guide axonal outgrowth and motility. B35 cells possess neuronal properties such as membrane excitability and expression of enzymes for neurotransmitter metabolism (Otey, Boukhelifa, and Maness 2003). BE(2)C is a subclone of the SK-N-BE(2) neuroblastoma cell line (Memorial Sloan Kettering Cancer Center 2019) derived from a metastatic site in human bone marrow (Biedler et al. 1978). BE(2) cells were found to possess short neurite-like outgrowths, neurotransmitter enzymes, and precursors to neuroblastoma compounds (Biedlere et al. 1978). Together, this shows that the cell lines used for cell studies possessed neuronal qualities.

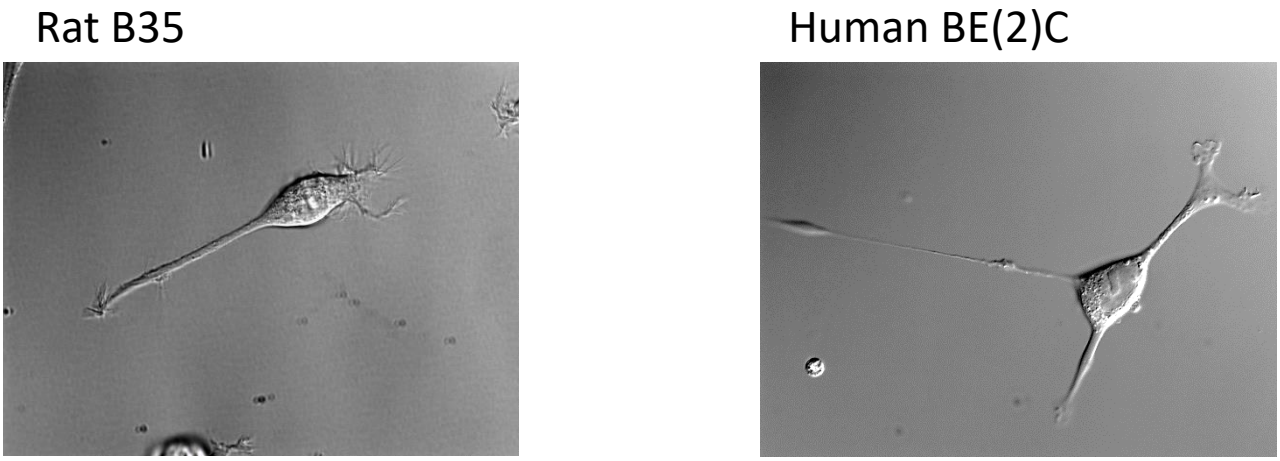

Figure 3. Images of neuroblastoma cells. DIC images of B35 rat neuronal cells (left) and BE(2)C human neuronal cells (right) grown in cell culture.

In this thesis, cancerous neuritic cell lines, neuroblastoma, were modified by employing CRISPR/Cas9 technology (Hall et al. 2017). These mutant cell lines have the *Mgat2* gene knocked out, which encodes for the enzyme GlcNAcT-II responsible for converting hybrid type glycans to complex, causing the cell to express predominantly hybrid type N-glycans. Our current research has found that glycosylation processing of Kv3.1 channels is vital for correct spatial localization of Kv3.1 in neurons and B35 neuroblastoma (Hall et al. 2013; Hall et al. 2017). In our past research, we have used B35 to study the effects the loss of *Mgat2* have on aberrant neuronal properties (Hall et al. 2017; Hall et al. 2018), but have not used a human cell model such as BE(2)C. We hypothesize that hybrid type N-glycans have a role in modulating cellular structure and function. The goal of this thesis is to study the role of glycans in cell behavior as well as, growth and development in vertebrates. Lectin blotting and flow cytometry will verify the successful knockout of *Mgat2* in human neuroblastoma. Anchorage independent growth assays will study the ability of cells to grow in suspension. Western blotting assays will show MMP-2 expression. Gelatinase assays will reveal MMP-2 activity. As well as CRISPR/Cas9 methods to generate other neuroblastoma knockout cell lines. A zebrafish model with the *Mgat1b* gene knocked out will be verified through genotyping and used to study the effects N-glycans have on vertebrae development.

Materials and Methods

Silencing of Mgat2

CRISPR-Cas9 technology was employed to silence the gene *Mgat2*. sgRNA oligonucleotides, 5'-CACCGTTCCGCATCTACAAACGGA-3' and 5'-AAACTCCGTTTGTAGATGCGGAAC-3' (Hall et al. 2016), were selected using the Zi-Fit Targeter software (Sander et al. 2007; Sander et al. 2010) and used to generate a rat neuroblastoma cell line with *Mgat2* silenced. After the phosphorylation and annealing of oligonucleotide, the double stranded gRNA was cloned into the pSpCas9(BB)-2A-Puro vector. The vector was transfected into rat B35 cells (NB) and human BE(2)C cells of 75-80% confluency using lipofectamine 2000. 1mL of FBS and antibiotic free DMEM containing 8 µg of vector and 15 µL Lipofectamine 2000 was added to each plate of cells. After a 5 hour incubation with the DMEM-DNA-lipid transfection solution, the cells were re-fed with 3 mL of complete DMEM. The transfected cells were then selected with 0.25 µg/mL puromycin for 48 hours. Genomic DNA of rat B35 cells was isolated, amplified, and sequenced to confirm the silencing of *Mgat2*. This cell line is referred to as NB(-*Mgat2*).

Rescue of HuNB(-Mgat2)

Human BE(2)C -*Mgat2* cell line was rescued by transient transfection with pCMVSport6 recombinant vector coding with mouse *Mgat2* cDNA (Hall et al. 2018). The vector was transfected into cells of 75-80% confluency using lipofectamine 2000. 1mL of FBS and antibiotic free DMEM containing 8 µg of vector and 15 µL Lipofectamine

2000 was added to each plate of cells. After a 5 hour incubation with the DMEM-DNA-lipid transfection solution, the cells were re-fed with 3 mL of complete DMEM.

Cell Culture

Human BE(2)C neuroblastoma (HuNB) cells were obtained from American Type Culture Collection and maintained in DMEM (Dulbecco's Modified Eagle Media) containing 10% FBS (fetal bovine serum), 50 U/mL penicillin, and 50 µg/mL streptomycin at 37°C under 5% CO_2, as previously described (Hall et al 2018). Cells were plated on 60 mm dishes and passaged every 3-5 days after 0.25% trypsin-EDTA treatment. Cell culture medium was changed every 2-3 days. Rat B35 neuroblastoma (NB) cells were obtained from American Type Culture Collection and maintained in DMEM (Dulbecco's Modified Eagle Media) containing 10% FBS (fetal bovine serum), 50 U/mL penicillin, and 50 µg/mL streptomycin at 37°C under 5% CO_2, as previously described (Hall et al 2018). Cells were plated on 60 mm dishes and passaged every 3-5 days after 0.05% trypsin-EDTA treatment. Cell culture medium was changed every 2-3 days.

Lectin Blotting

Whole cell lysates were collected from 80-100% confluent 60 mm culture dishes. Cells were washed with PBS and lysed with 200 µL of RIPA (Radioimmunoprecipitation assay) buffer. Cells were taken up into a 1 mL syringe with a 22-gauge needle. Cells were sheered through use of syringe and collected in a microcentrifuge tube. Sheered cell contents were incubated on ice for 45 minutes and then centrifuged at 4°C at 20000 x g for 20 minutes. Supernatant was then collected as whole cell lysate and stored at -

80°C until time to acquire protein concentration through Lowry assay. Samples then had 2X reducing SDS-PAGE sample buffer added to them, as previously mentioned (Hall et al. 2014).

Reduced whole cell lysate samples were then subjected to electrophoresis for 90-110 minutes at 20 mA on 10% SDS gels. Proteins were then transferred to Immobilon-P PVDF membranes at 250 mA for 120-150 minutes. Blots were incubated at room temperature for 20-30 minutes in blocking buffer (PBS, 5% non-fat dry milk (Bio-Rad) with 0.05% Tween 20) on a rotating platform. Blot was then incubated overnight at 4°C in Biotin-conjugated *Phaseolus vulgaris* Erythoagglutinin (E-PHA), *Phaseolus vulgaris* Leucoagglutinin (L-PHA), or *Galanthus nivalis* lectin (GNL) to probe membranes containing separated glycosylated proteins. Blots were then washed four times in PBS plus 0.05% Tween 20 and developed with ImmunO alkaline phosphatase substrate, as previously mentioned (Hall et al. 2015).

Lectin Flow

Human BE(2)C cells were incubated with 10 µg/mL of a fluorescein tagged lectin *Phaseolus vulgaris* Erythoagglutinin (E-PHA), *Phaseolus vulgaris* Leucoagglutinin (L-PHA), or *Galanthus nivalis* lectin (GNL) at room temperature for 15 minutes. A FACS Vantage flow cytometer was then used with 488 nm laser excitation and emission centered at 530 nm to obtain fluorescence intensity, previously mentioned (Hall et al. 2017). The mean fluorescence was found from histogram plots of fluorescence emission.

Total membrane isolation and glycosidase digestions

Human BE(2)C cells expressing wild type and N220Q/N229Q Kv3.1b EGFP fusion proteins were homogenized (30-40 strokes) in 3 mL of lysis buffer; 250 mM sucrose, 5 mM EDTA, protease inhibitor cocktail set III 1:500. The homogenate was centrifuged in an Eppendorf F-45-30-11 rotor at 2000 x g for 10 min at 4°C. The supernatant was then centrifuged at 100000 x g for 1 hour at 4°C in an AH650 rotor. The pellet formed from the highspeed spin of the supernatant was then resuspended in 150 µL of lysis solution. The protein concentration was determined by Lowry assay. Samples were stored at -80°C until needed, as mentioned prior (Hall et al. 2017).

Total membranes containing wild type and N220Q/N229Q Kv3.1b EGFP fusion proteins were treated with PNGase F (20 U/ µL), Endo H (50 U/ µL), or Neuraminidase (0.83 / µL) in New England Biolabs supplied buffers, as previously (Hall et al. 2017). Reactions were carried out overnight at 37°C and stopped by the addition of 2X reducing SDS-PAGE sample buffer.

Kv3.1b western blot

Purified samples of Kv3.1b proteins in reducing SDS sample buffer were subjected to electrophoresis for 90-110 minutes at 20 mA on 10% SDS gels. Proteins were then transferred to Immobilon-P PVDF membranes at 250 mA for 120-150 minutes. Blots were incubated at room temperature for 20-30 minutes in blocking buffer (PBS, 3% BSA with 0.1% Tween 20) on a rotating platform. Blot was then incubated overnight at 4°C in mouse anti-Kv3.1b antibody. Blots were then washed three times in

PBS plus 0.05% Tween 20 and developed with ImmunO alkaline phosphatase substrate, as described previously (Hall et al. 2018).

Human MMP-2 Western blot

Human neuroblastoma cells were grown to confluency in a T-75 culture flask at 37°C under 5% CO_2. 30mL of serum free DMEM media was added to the dishes and incubated for 48 hours at 37°C under 5% CO_2. Media was then collected and concentrated to similar levels and frozen at -80°C until time to acquire protein concentration through Lowry assay. Samples then had 2X reducing SDS-PAGE sample buffer added to them. Proteins in 2X reducing SDS sample buffer were subjected to electrophoresis for 90-110 minutes at 20 mA on 10% SDS gels. Proteins were then transferred to Immobilon-P PVDF membranes at 250 mA for 120-150 minutes. Blots were incubated at room temperature for 20-30 minutes in blocking buffer (PBS, 3% BSA with 0.1% Tween 20) on a rotating platform. proteins from media were incubated in rabbit primary anti-MMP-2 antibodies. Blots were then washed three times in PBS plus 0.05% Tween 20, incubated in rabbit secondary and mouse secondary antibodies, washed again, and then developed with ImmunO alkaline phosphatase substrate.

Rat MMP-2 Western blot

Rat neuroblastoma cells were grown to confluency in a 100 mm culture dish at 37°C under 5% CO_2. 10 mL of serum free DMEM media was added to the dishes and incubated for 48 hours at 37°C under 5% CO_2. Media was then collected and concentrated to 200 µL using a Vivaspin20 and frozen at -80°C until time to acquire protein concentration through Lowry assay. Cells were washed with PBS and lysed with

400 µL of RIPA buffer. Cells were taken up into a 1 mL syringe with a 22-gauge needle. Cells were sheered through use of syringe and collected in a microcentrifuge tube. Sheered cell contents were incubated on ice for 45 minutes and then centrifuged at 4°C at 20000 x g for 20 minutes. Supernatant was then collected as whole cell lysate and stored at -80°C until time to acquire protein concentration through Lowry assay. Samples then had 2X reducing SDS-PAGE sample buffer added to them, as previously described (Hall et al. 2018).

Proteins in 2X reducing SDS sample buffer were subjected to electrophoresis for 90-110 minutes at 20 mA on 10% SDS gels. Proteins were then transferred to Immobilon-P PVDF membranes at 250 mA for 120-150 minutes. Blots were incubated at room temperature for 20-30 minutes in blocking buffer (PBS, 3% BSA with 0.1% Tween 20) on a rotating platform. Blot was then cut in half. Proteins from whole cell lysates were incubated overnight at 4°C in mouse primary anti-beta tubulin while the proteins from media were incubated in rabbit primary anti-MMP-2 antibodies. Blots were then washed three times in PBS plus 0.05% Tween 20, incubated in rabbit secondary and mouse secondary antibodies, washed again, and then developed with ImmunO alkaline phosphatase substrate.

Independent Anchorage Growth Assay

1% Noble agar in complete 2X DMEM was heated to a liquid state and 1.5 mL was aliquoted per well in a 6 well plate. The agar was cooled at room temperature for 30 minutes allowing it to solidify and form the base layer. Equal parts of cell suspension in 1X DMEM mixed with 0.6% Noble agar was added to the top of the base layer. A thin layer of 1X DMEM was then added above top Noble agar layer, as previously

mentioned (Hall et al. 2018). The cells were cultured at normal growth conditions for 14 days. Images were acquired using 4X objective on an Olympus IX73 microscope. ImageJ software was then used to measure the number of cell colonies and cell colony area.

Wound Healing Assay

Cell migration experiments were done as previously described (Hall et al. 2018). Human parental and N-glycosylation mutant neuroblastoma cell lines were seeded in equal concentrations onto a 60 mm CellBind culture dishes. After cells were grown to confluency, complete DMEM was removed from dishes and scratches were made through the cell layer using a beveled 200 µL pipet tip. Cell were rinsed with complete DMEM and re-fed with 3 mL of complete DMEM. Using an Olympus IX 50 microscope at 10X objective, images of the wounds were taken at 0 hours and then again after 19 hours of incubation at normal growth conditions. ImageJ software was utilized to measure the change in distance between the opposite sides of the wound. The percent wound closure was found by taking the difference in wound closure between the initial width (0 hours) and final width (19 hours) of the wound and dividing by the initial wound width.

Gelatin Zymography

Gelatin zymography assays were conducted as described by manufacturer, with slight variation (abcam). Samples of concentrated conditioned serum free media were adjusted to the same protein concentration. 5X non-reducing buffer (4% SDS, 20% glycerol, 0.01% bromophenol blue, 125 mM Tris-HCl pH 6.8) was added to the samples.

For each sample, 3 different protein concentrations were used to measure MMP-2 protein activity. Samples were loaded into a 1 mm thick 10% acrylamide gel containing gelatin (1.5 M Tris pH 8.8, acrylamide, water, 4 mg/mL gelatin, 10% SDS, 10% APS, TEMED). Gel electrophoresis was conducted at 20 mA. After gel electrophoresis, the gel is washed with washing buffer (2.5% Triton X-100, 50 mM Tris-HCl pH 7.5, 5 mM $CaCl_2$, 1 µM $ZnCl_2$, water) twice for 30 minutes. The gel was then rinsed for 5-10 minutes in incubation buffer (1% Triton X-100, 50 mM Tris-HCl, 5 mM $CaCl_2$, 1 µM $ZnCl_2$, water) at 37°C with slight agitation. Incubation buffer was replaced with fresh buffer and gel was incubated for 24 hours at 37°C with slight agitation (100 rpm in a shaking incubator). The gel was then stained with Coomassie stain (Methanol, Acetic acid, water, Coomassie Blue) for 30 minutes to an hour whilst on a rotator. Gel is then destained with destaining solution (40% Methanol, 10 % Acetic acid, water) until white bands are clearly visible against a blue background.

Zebrafish Genotyping

Individual zebrafish were isolated in tanks and treated with MS222 (Tricaine methanesulfonate) solution to sedate and anesthetize them. Part of the caudal fin is then clipped using clean scissors and placed in a microcentrifuge tube. 25 µL of 50 mM NaOH is then added to the fin clips and heated to 99°C using an MJ Research MiniCycler for 15 minutes or until dissolved. DNA from the dissolve fin clip is then amplified through PCR, Polymerase Chain Reaction, as previously described (Meeker et al. 2007). 10 µL PCR reactions were carried out using a Bio-Rad iCycler (Denaturing at 95°C, Annealing at 58°C, Elongation 72°C). Restriction reactions using BclI were then carried out at 37°C to genotype individual zebrafish. Product was then run on an 1.5%

agarose gel with Ethidium Bromide to determine if PCR product could be cleaved. Uncut product indicates a homozygous mutant (1 band), fully cut product indicates a homozygous wildtype (2 bands), and partially cut product indicates a heterozygous fish (3 bands).

Zebrafish embryo viability

A male and female zebrafish were isolated in 1 liter breeding tanks separated by a plastic divider the night before crosses ensued. Crosses of wild type with wild type, heterozygous mutant with heterozygous mutant, and homozygous mutant with homozygous mutant were performed during the early morning, when the lights in the fish facility first turn on. Embryos were collected and washed 3 times with egg water (0.294 g NaCl, 0.013 g KCl, 0.049 g $CaCl_2 \cdot 2H_2O$, 0.081 g $MgSO_4 \cdot 7H_2O$, 0.5 g Methylene blue, Fish-system water). Embryos were stored in 100 mm culture dishes submerged in egg water at 29°C. Viable embryos were counted at 0, 4, 8, 12, 18, and 24 hours past fertilization. Viable embryos were determined by inspection through use of dissecting microscopes.

Results

Part 1: Cell Model

Characterization of Cell Model and Tumorigenicity

In order to compare the cellular roles of hybrid type N-glycans to complex type N-glycans, N-glycosylation mutants were created through the employment of CRISPR-Cas9. A human neuroblastoma (HuNB) cell line and a rat neuroblastoma (NB) cell line (Hall et al. 2017) were altered by silencing the *Mgat2* gene, responsible for encoding the enzyme GlcNAcT-II which converts hybrid type N-glycans to complex type. This was done through the insertion of a cytosine after the 22nd nucleotide in the *Mgat2* gene causing a frameshift mutation, shown by the red arrow in Figure 4. The N-glycosylation mutants, HuNB(-*Mgat2*) and NB(-*Mgat2*), should therefore predominately express hybrid type N-glycans while the parental cell lines, HuNB and NB, express predominately complex type N-glycans.

A.

HuNB: atg agg ttc cgc atc tac aaa cgg aag gtg cta atc ctg acg

HuNB(-*Mgat2*): atg agg ttc cgc atc tac aaa ccg gaa ggt gct gat cct gac

B.

NB: atg agg ttc cgc atc tac aaa cgg aag gtg cta atc ctg acg

NB(-*Mgat2*): atg agg ttc cgc atc tac aaa ccg gaa ggt gct gat cct gac

Figure 4. Silencing of *Mgat2*. Human and rat neuroblastoma cell lines were created through use of CRISPR-Cas9. The coding sequence of the *Mgat2* gene from nucleotide 1 to 42 is shown. The *Mgat2* gene is silenced through the insertion of a cytosine residue after the 22nd nucleotide, shown by red arrow, resulting in a frame shift mutation in both the human cell line (A) and the rat cell line (B).

To verify that the predominate N-glycans expressed in the HuNB(-*Mgat2*) are hybrid type N-glycans, lectin binding of this cell line was compared to the parental cell line HuNB. Fluorescently labelled lectins were bound to HuNB and HuNB(-*Mgat2*) cell lines and the level of fluorescent intensity was measured through flow cytometry. The lectins used were *Phaseolus vulgaris* Erthroaglutinin (E-PHA), *Phaseolus vulgaris* Leucoagglutinin (L-PHA), and *Galanthus nivalis* Lectin (GNL). E-PHA has a higher binding affinity for complex N-glycans with bisecting N-acetylglucosamine over hybrid bisecting N-glycans (Narasimhan, Freed, and Schachter 1986). L-PHA has a higher binding affinity for complex N-glycans over hybrid and oligomannose N-glycans (Narasimhan, Freed, and Schachter 1986). GNL has a higher binding affinity for hybrid N-glycans over complex (Cummings and Etzler 2009). The flow cytometry plots, shown in Figure 5A, indicate that L-PHA and E-PHA bind to the cell surface of HuNB cells with a higher affinity than to HuNB(-*Mgat2*) cells. GNL binds to the cell surface of HuNB cells with less affinity than HuNB(-*Mgat2*) cells. Figure 6A compares the average fluorescent intensity of the fluorescently labelled lectins bound to the cell surface of the parental and mutant cells. A significant difference was found across all lectins with E-PHA and L-PHA binding with a higher affinity to HuNB cells and GNL binding with a higher affinity to HuNB(-*Mgat2*) cells. Figure 6B shows the ratio of the average fluorescent intensity of the parental to the mutant cell line. The results show that E-PHA binds to the HuNB cells with a binding affinity seven fold more than the HuNB(-*Mgat2*) cells, L-PHA binds to HuNB cells with a binding affinity nine fold more than HuNB(-*Mgat2*) cells, and GNL binds to HuNB with less than half the binding affinity as HuNB(-*Mgat2*) cells. These results support that the *Mgat2* gene is silenced in the HuNB(-*Mgat2*) and that the cell line predominately expresses hybrid type N-glycans.

A.

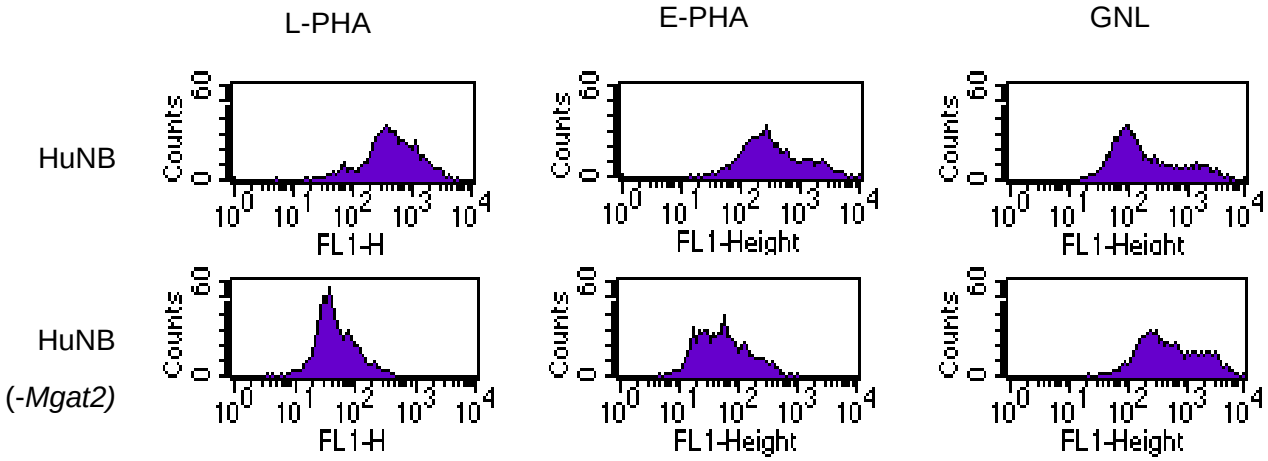

B.

Lectin Binding Affinity	
L-PHA	Complex>>hybrid>oligo mannose
E-PHA	Bisecting
GNL	Oligomannose>hybrid> >complex

Figure 5. Characterization of a human N-glycosylation mutant through flow cytometry. Flow cytometry plots of three fluorescently labelled lectins, E-PHA, L-PHA, and GNL binding each of the human cell lines is shown in panel A. Table representing the lectin and its binding affinity shown in panel B.

A.

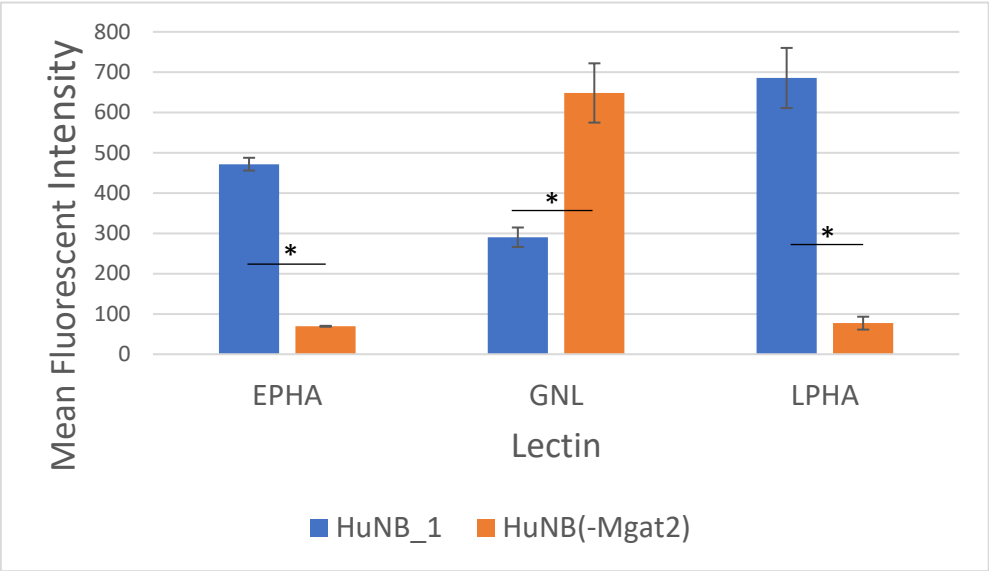

B.

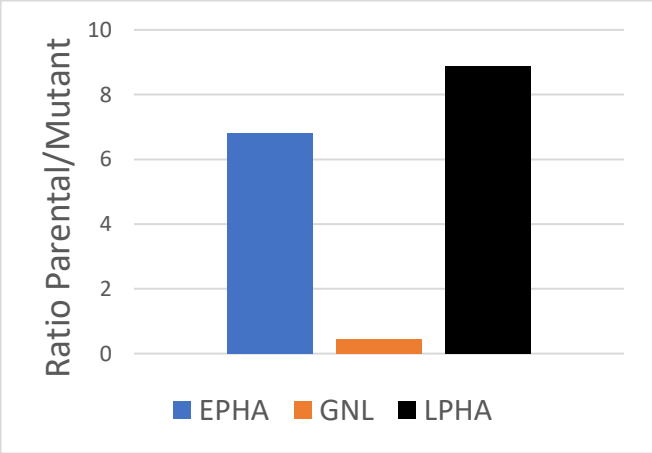

Figure 6. Analysis of fluorescently labelled lectins. Mean fluorescence intensity of human neuroblastoma cell lines (A). * denotes a significant difference at $p<0.05$. Experiments were done in three sets of triplicate and analyzed through student t-test. The ratio of the mean fluorescence of the parental cell line to the mutant cell line shows the fold difference between lectin binding (B).

To further verify that the type of N-glycans on the cell surface of the N-glycosylation mutant HuNB(-*Mgat2*) was due to the loss of *Mgat2,* lectin blotting was conducted with whole cell lysates from the HuNB, HuNB(-*Mgat2*), and also a HuNB(-*Mgat2*) cell line transiently transfected with *Mgat2,* termed HuNB(+/-*Mgat2*) (Figure 7). The lectins L-PHA, E-PHA, and GNL were used to probe separated proteins from the whole cell lysates and determine the binding affinities of the lectins for N-glycans attached to surface proteins. L-PHA was used since it has a higher binding affinity for complex type N-glycans over hybrid type. Bands of the highest intensity were found in the lane containing proteins from HuNB, while the intensity of the bands in the lane containing the HuNB(-*Mgat2*) were decreased. E-PHA was used since it has a higher binding affinity for complex type N-glycans with bisecting N-acetylglucosamine over hybrid type N-glycans with bisecting N-acetylglucosamine. Bands with high intensity were found in the lane containing HuNB, the lane with the least intense bands contained HuNB(-*Mgat2*). GNL was used since it has a higher binding affinity for hybrid type N-glycans over complex type. Numerous bands with high intensity were found in the lane containing HuNB(-*Mgat2*) and the lane with the least intense bands contained HuNB. The HuNB(-*Mgat2*) cell line transiently transfected with *Mgat2* showed band intensities more similar to those of the HuNB cell line than HuNB(-*Mgat2*). The Coomassie blue stained gel showed that the levels of proteins loaded per well were similar for each lectin blot. These results, taken with the results of the lectin flow cytometry studies indicate that knock out of *Mgat2* was successful and that the HuNB(-*Mgat2*) cell line predominately expresses hybrid type N-glycans. Therefore, the cellular differences between the cell lines should be due to the N-glycans predominantly expressed.

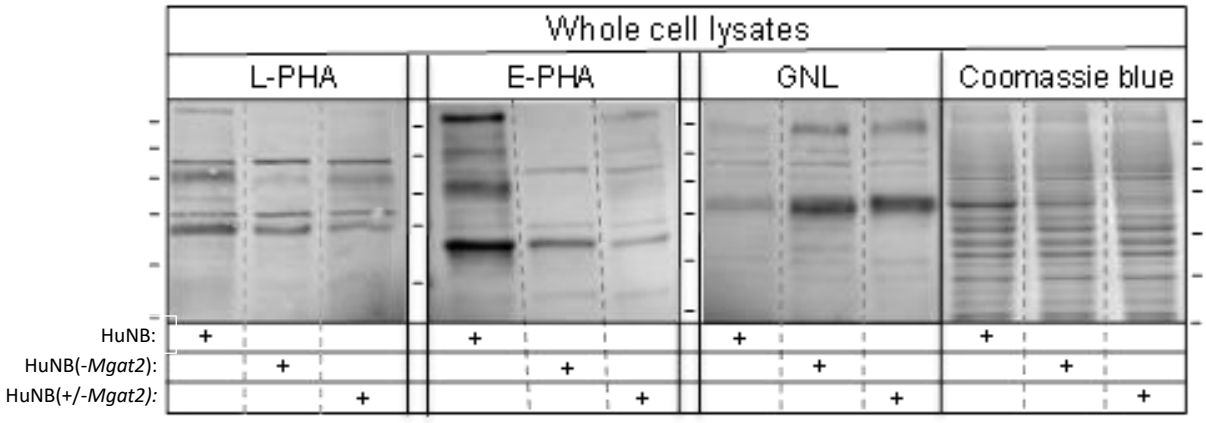

Figure 7. Characterization of human cell lines through lectin blotting. Lectin blots of whole cell lysates show the predominate N-glycans present within cell lines. The far right panel shows similar levels of proteins were evaluated by Coomassie blue. Plus signs signify the cell line examined. Lines denote the molecular weight in kilodaltons from top to bottom: 250, 150, 100, 75, 50, 37, 25 and 20. Lectins were each repeated three times.

The Kv3.1b channel has been found to possess two highly conserved glycosylation sites, N220 and N229, at the S1-S2 linker (Shi and Trimmer 1999; Brooks, Corey, and Schwalbe 2006). Studies have shown that the alteration of these glycosylation sites in Kv3.1b results in slower activation and deactivation rates of the channel when compared to a fully glycosylated Kv3.1 within neuronal rat cells (Hall et al. 2011; Hall et al. 2017). The migration of these neurons also slowed as the glycosylation sites became more vacant (Hall et al. 2011). These results are indicative that the glycosylation of the Kv3.1 glycoprotein plays a crucial role in the conducting and non-conducting properties of the channel. To further demonstrate that N-glycosylation processing is altered in the HuNB(-*Magt2*) cell line we characterize the Kv3.1b channel in the HuNB, HuNB(-*Mgat2*), and HuNB(+/-*Mgat2*) cell lines which heterologously express Kv3.1b proteins. Kv3.1 *N*-glycosylation mutants, N220/9Q, were constructed by highly conserved mutations of the Asn residues to Gln residues (Brooks, Corey, and Schwalbe 2006). Total membranes of the various cell lines were isolated, and partially purified Kv3.1b samples were then analyzed by Western blots. The wild type Kv3.1 expressed in the HuNB, HuNB(-*Mgat2*), and HuNB(+/-*Mgat2*) cell lines migrated as a doublet with a predominant slower band and a fainter fast band migrating at ~80 kDa, shown in Figure 8A. The faster band represents the attachment of oligomannose N-glycans (Cartwright, Corey, and Schwalbe 2007), while the slower upper band represents the attachment of N-glycans corresponding to the predominate N-glycans expressed. The upper band of Kv3.1b belonging to HuNB migrated the slowest (~98 kDa) due to the attachment of complex type N-glycans. The upper band of Kv3.1b belonging to HuNB(-*Mgat2*) migrated the quickest (~88 kDa) due to the attachment of

hybrid type N-glycans. The HuNB(-*Mgat2*) cell line transiently transfected with *Mgat2* showed a much different upper band migrating at a rate in between the HuNB and HuNB(-*Mgat2*) Kv3.1b proteins, due to the attachment of hybrid and complex type N-glycans. When the glycosylation sites were abolished, represented by the N220/9Q samples, a single band was detected (~75 kDa) migrating at the fastest rate. To further characterize the Kv3.1b proteins expressed in the HuNB and HuNB(-*Mgat2*) cell lines, the partially purified Kv3.1b proteins underwent glycosidase treatment, shown in figure 8A&B. PNGase F which digests all glycans, neuraminidase which digests sialic acid residues, and Endo H which digest oligomannose were used on the Kv3.1b proteins. When compared to the untreated sample, the upper bands were sensitive to neuraminidase and PNGase F and resistant to Endo H. The lower bands resisted neuraminidase and were sensitive to PNGase F and Endo H. These results indicate that the upper band of the Kv3.1b found in HuNB and HuNB(-*Mgat2*) cells contained sialylated N-glycans and the lower band contains oligomannose N-glycans. Taken together, the Western blots and lectin binding studies strongly support that *Mgat2* was silenced and therefore the parental cell line expresses predominately complex while the mutant expresses predominately hybrid type N-glycans.

A.

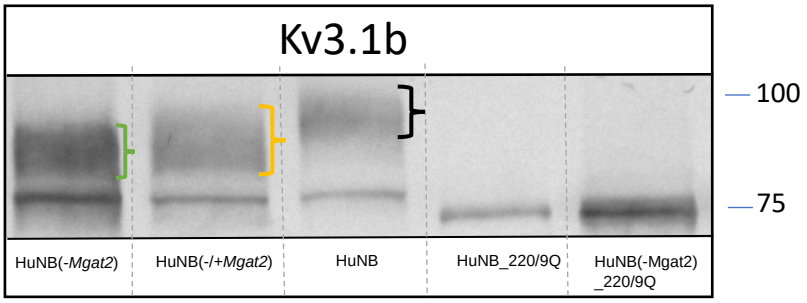

B.

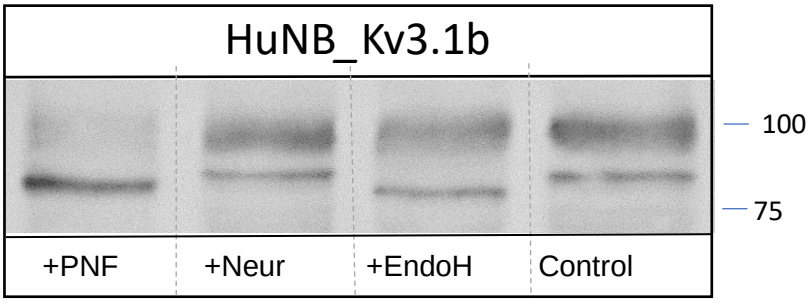

C.

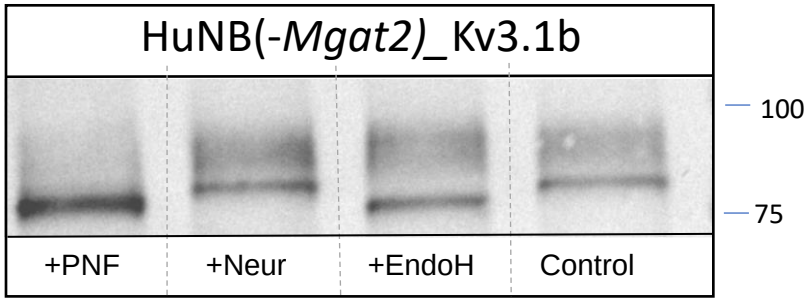

Figure 8. Characterization of Kv3.1b proteins expressed in human neuroblastoma cells. Western blots of total membranes of the parental (HuNB), mutant (HuNB(-*Mgat2*)), rescued mutant (HuNB(+/-*Mgat2*)), and parental and mutant N220Q/N229Q Kv3.1b proteins. Brackets denote the Kv3.1b protein with complex/hybrid type N-glycans (A). Glycosidase treatment of the glycosylated and unglycosylated Kv3.1b proteins resulted in immunoband shifts allowing for the assignment of N-glycan types (B and C). The numbers and lines adjacent to Westerns represent the Kaleidoscope markers in KDa. Westerns were repeated three separate times.

The ability of cells to grow independent of attachment is connected to tumorigenic and metastatic potentials, and is used as an indicator for the transformation of cancerous cells (Mori et al 2009). To determine the role complex type N-glycans have in the ability of neuroblastoma cells to proliferate independent of cellular attachment, an anchorage-independent cell growth assay was conducted. Cells were grown in soft agar suspension for 14 days under normal culture conditions and then images of cell colonies were obtained from 3 wells for each of 3 experiments. Representative micrographs of the cell colonies are shown in Figure 9A. HuNB cells expressing predominately complex type N-glycans formed colonies significantly larger than that of the HuNB(-*Mgat2*) cells, shown in Figure 9B. HuNB cells were also found to form significantly more cell colonies than the HuNB(-*Mgat2*) cells. These results indicate that the presence of complex type N-glycans contribute to an increase in tumorgenicity.

A.

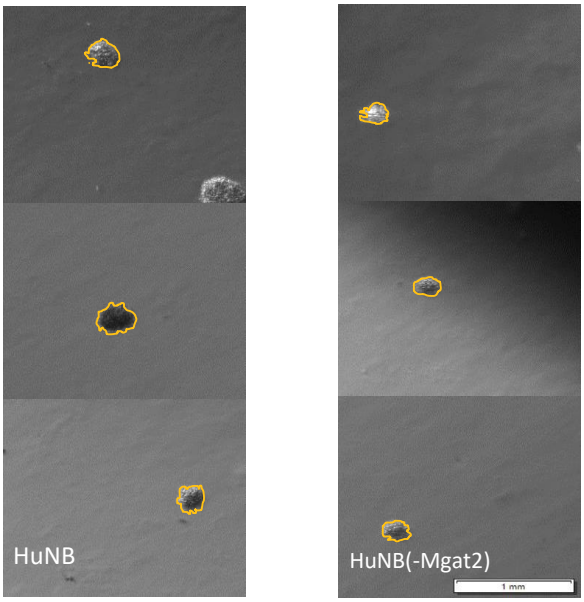

B.

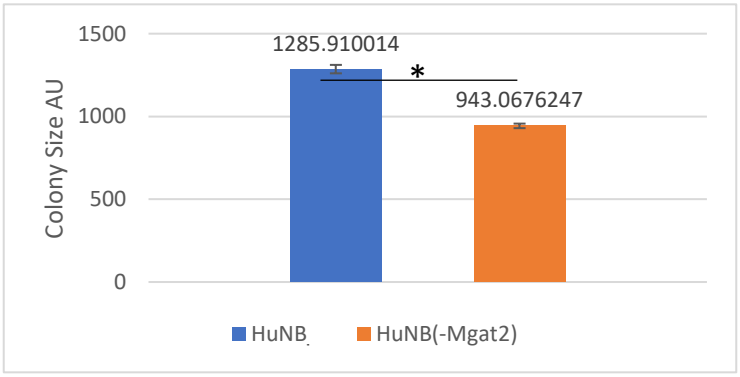

C.

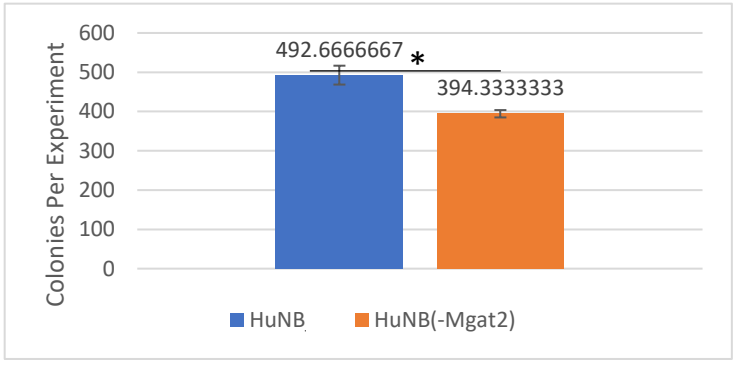

Figure 9. Tumorigenic growth is lessened by the loss of *Mgat2*. Micrographs of colony formation of HuNB (left panels) and HuNB(-*Mgat2*) (right panels) grown in agar suspension for 14 days under normal culture conditions (A). Graph shows the average size of colonies formed after 14 days of growth (B). Graph shows the average number of colonies formed per experiment (C). * denotes a significant difference at $p<0.05$. Experiments were done in three sets of triplicate and analyzed through student t-test.

Cell migration is critical in the metastatic spread of cancer cells and the formation of metastasis. Migratory cancer cells can undergo molecular and cellular changes by remodeling their cell-cell and cell-matrix adhesion (Yilmaz and Christofori 2010). To determine the role complex type N-glycans play in the migratory ability of neuroblastoma cell, wound healing assays of the HuNB and HuNB(-*Mgat2*) cell lines were conducted. Scratches were made on a monolayer of similarly confluent cell culture plates and incubated at normal cell culture conditions. Images of the cell wounds were taken at 0 hours and 19 hours after initiation of scratches. The images shown in Figure 10A represent one scratch for each cell line from the four independent experiments. A bar graph shown in Figure 10B demonstrates that the average percent wound closure of the HuNB(-*Mgat2*) cells were slightly, but significantly faster than the HuNB cells. These results indicate that the elimination of complex type N-glycans plays a role in the enhancement of the cell migratory rate for neuroblastoma cells.

A.

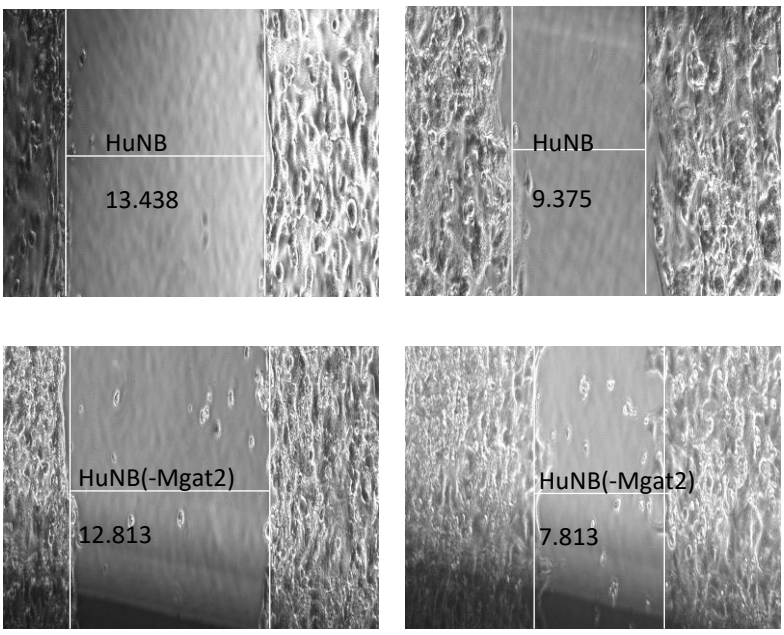

B.

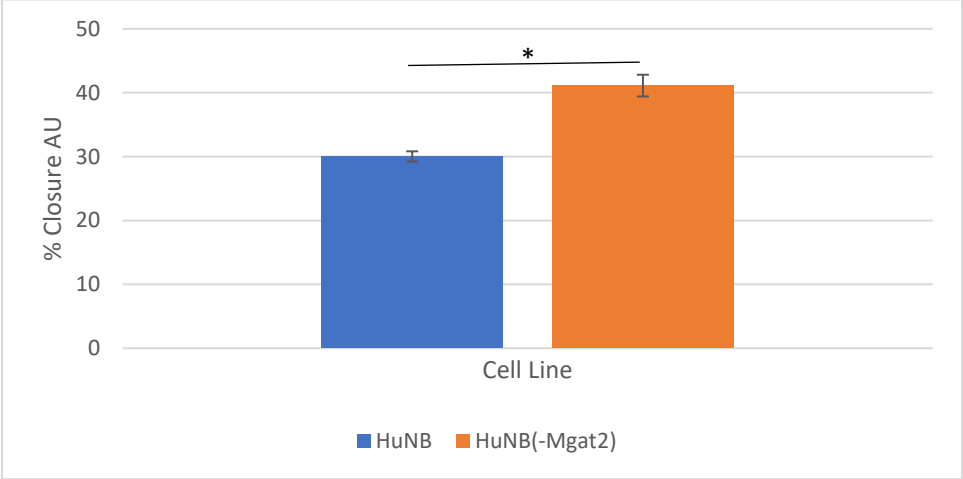

Figure 10. Cell migration is enhanced through knockout of *Mgat2*. Micrographs of wound healing assay at 0 hr and 19 hr after the initial scratch in human NB cells (A). Graph shows the average ratio of wound closure to initial wound size (B). * denotes a significant difference at $p<0.05$. Experiments were repeated independently four times.

Some hallmarks of cancer include migration, invasion, and metastasis. Crucial molecules throughout these processes are matrix metalloproteases (MMPs) (Gialeli, Theocharis, & Karamanos 2011). To determine how the loss of complex type N-glycans affect the expression of MMP-2, serum free media containing secreted MMP-2 was analyzed by Western blots. Cells were grown to similar confluency in serum free media under normal culture conditions for 48 hours. Serum free media was then collected and concentrated to similar volumes. Western blot of MMP-2 expression shows a predominate intense band for the HuNB cell line and a much fainter band for the HuNB(-*Mgat2*), as shown in in Figure 11A. A Coomassie blue stained gel shown in Figure 11B shows similar levels of protein was loaded per well. This result shows that the loss of complex type N-glycans leads to a decreased expression of MMP-2.

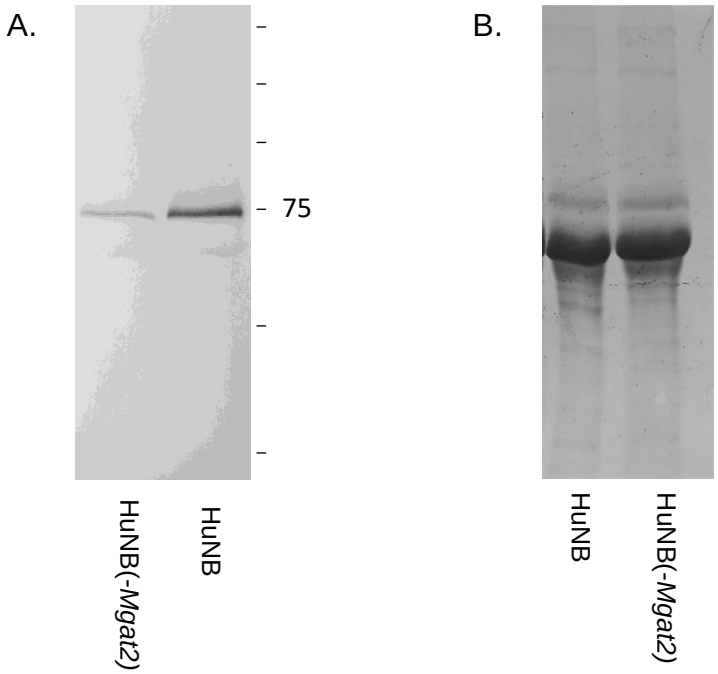

Figure 11. Decreased MMP-2 expression by loss of *Mgat2* in human neuroblastoma. Western blot of MMP-2 secreted into serum free culture media from HuNB and HuNB(-*Mgat2*) cell lines (A). Coomassie blue of media proteins (B). The numbers and lines adjacent to Westerns represent the Kaleidoscope markers in KDa. Westerns were repeated three times.

To further verify that decreased MMP-2 expression is due to the loss of complex type N-glycans, MMP-2 expression and activity was studied in rat neuroblastoma cell lines NB and NB(-*Mgat2*) through Western blot and zymography analysis. Cells were grown to similar confluency in serum free media under normal culture conditions for 48 hours. Serum free media was then collected and concentrated to similar volumes and whole cell lysates of the cells were harvested. A Coomassie blue stained gel shows that similar levels of proteins were loaded per well for the whole cell lysates (lanes 1&2) and serum free media (lanes 4&5), as shown in the first panel. Western blot analysis of MMP-2 expression shows that NB cells with predominately complex type N-glycans (lane 1) express MMP-2 at a higher level than the NB(-*Mgat2*) cells with predominately hybrid type N-glycans (lane 2), as shown in the second panel. Gelatin zymography assays were used to measure proteolytic activity of MMP in the serum free media. An inverted image of a zymography gel, shown in the third panel, reveals that NB cells exhibit higher MMP activity than the NB(-*Mgat2*) cells. The molecular weight of MMP-2 shown by Western blot is similar to that of the MMP identified on the gelatinase gel, suggesting the MMP activity is that of MMP-2. A Western blot using anti-β-Tubulin on the whole cell lysates was used to show that similar amounts of cells were present at the time the serum free media was harvested. Results indicate that the loss of complex type N-glycans leads to a decreased expression and activity of MMP-2.

A.

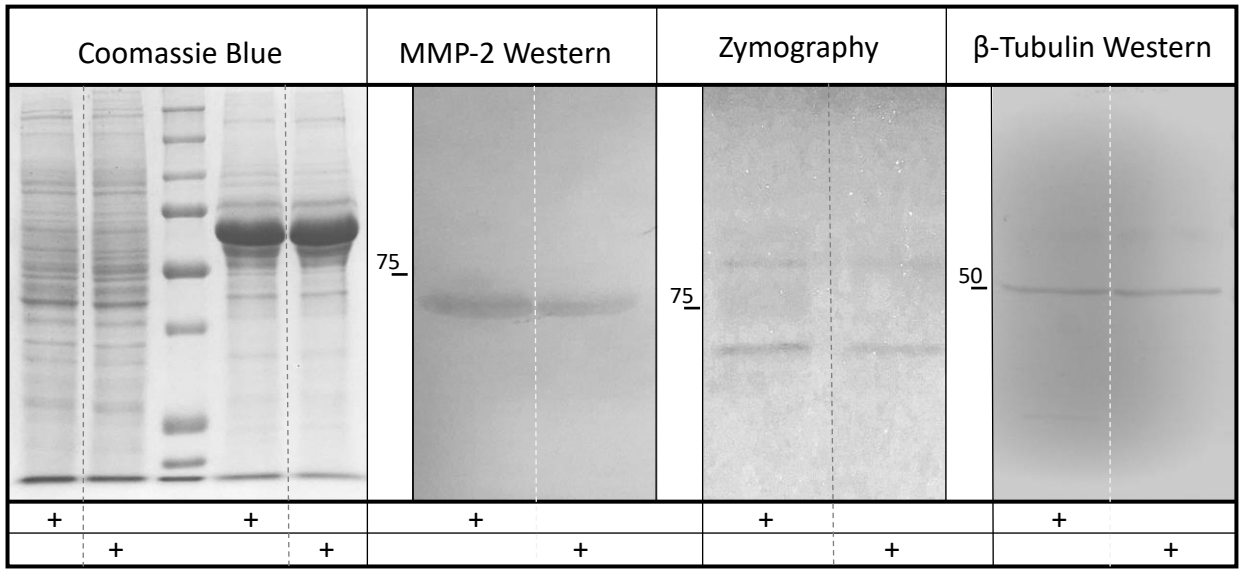

Figure 12. Loss of complex N-glycans results in decreased expression of MMP-2 and activity. Coomassie blue (far left panel) of whole cell lysates (lanes 1&2) and serum free culture media (lanes 4&5) shows similar levels of proteins were evaluated. Western blots of MMP-2 (mid-left panel) secreted into serum free culture media from NB and NB(-*Mgat2*) cell lines. Zymography (mid-right panel) measuring proteolytic activity of MMP-2 in serum free culture media. β-Tubulin Western blots (far right panel) of whole cell lysates show similar number of cells were seeded. The numbers and lines adjacent to westerns represent the Kaleidoscope markers in KDa. Plus signs indicate cell line. Experiments were repeated three separate times.

Taken together, these results support that the N-glycosylation pathway was altered by the loss of *Mgat2* through lectin binding studies and Western blotting. Complex type N-glycans were predominately expressed in the HuNB cell line and hybrid type N-glycans were predominately expressed in the HuNB(-*Mgat2*) cell line. Analysis of the tumorigenic properties of these neuroblastoma cell lines revealed that the substitution of complex type N-glycans for hybrid suppressed colony formation, suppressed MMP-2 expression, and increased cell migration. These results suggest that the lack of complex type N-glycans lessen aberrant neuronal properties, overall.

Part 2: Multicellular Organism

Loss of Hybrid and Complex Type N-glycans in a Zebrafish Model

In order to study how the increase of oligomannose type N-glycans affect growth and development, particularly neuronal function in a multicellular organism, the CRISPR-Cas9 technique was employed to silence the *Mgat1b* gene, in zebrafish. The *Mgat1b* fragment (576nt), shown in Figure 13, contains the gRNA sequence (20nt), which has a restriction site Bcl2, indicated by arrows and highlighting. This fragment will be amplified to identify indels. The Bcl2 site, when digested with the restriction enzyme BclI, will allow the *Mgat1b* fragment to be cut into two fragments, 204 and 372 base pairs. However, when an indel occurs the Bcl2 site will be altered, so the size of the fragment will be 576nt. DNA of embryos microinjected with RNA and caspase9 will be isolated, amplified, and treated with the restriction enzyme BclI. If some of the DNA is not digested by the BclI, then we know that the sequence at the Bcl2 site was modified and that the gRNAs cause indels. Next, microinjected embryos will be allowed to develop to adults. DNA from tail clips of adult fish will then be isolated, amplified, and digested. In some cases, samples of uncut DNA will be sent off for sequencing to verify and identify nucleotides that have been altered.

A.

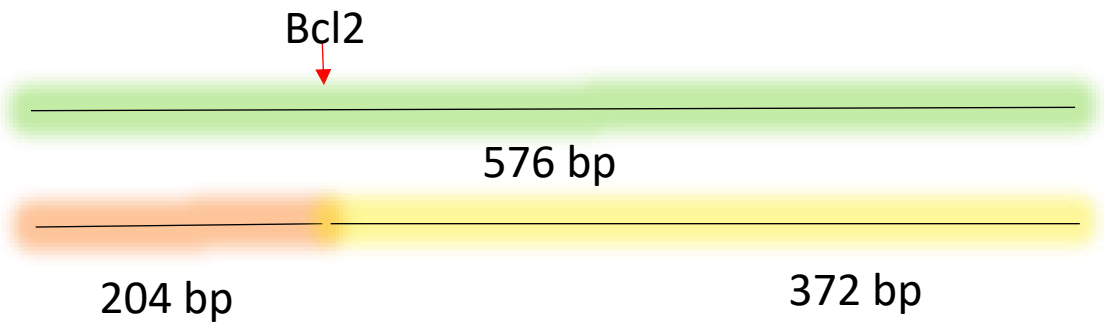

B.

5′ GCCATG GTTCGCAAGAAAGG ATCTCTTATTTTGTGCGGAGCTTTTTTGTTTGTCGCCTGGA
ACGCCTTGCTCCTCCTCTTCTTATGGGGGAGGCCTCCCATTGGTCGACTT GGGGAGGGAGGT G
GAGCCGAACCAGGGGCCGGAGAAGAGTGGGGAGCAGGAAAGTCAAAAGTGGGTGGAGCTAACGG
ATTGGCCGGTGAAGTGATCAGAT TGGCTGAAGAAGTAGAATCGGAACTGGAGACTCAAAAGAAG
CTCCTCAAACAAATTCAAAGCCACAGAGAACTATGGGAACAGCGGAAGGAACTGGAAAAGAGAG
AATCGGAGGACACGAAGGATGAAAAGATCGACGTAGAGCCTAAAAAGCCTAGGCAGATTCCTGC
AG TAC ATCTAAGTCATAAAGTGGTAGAAT ATGCACAAACTGTTACGAAAAAAAC GCAGACTTT
AATG GTCACGCCGCCTCAGCTGGTCATGA AGGAGCAGGAAACAGACCAAAAGAACAAGCAAAT
GATGGAAGATCAACTAGGCCTTACTACACCAAGCCCTCAAATCATTATCCCAATTCTGGTCATT
GCCTG-3′

C.

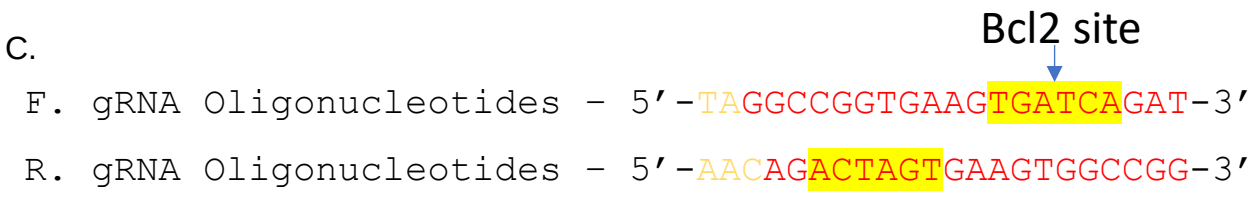

Figure 13. Design for Zebrafish knockout of *Mgat1b.* *Mgat1b* fragment shown to be 576 base pairs with a Bcl2 site indicated by the red arrow. Bcl2 site cuts *Mgat1b* into two fragments, 204 and 372 base pairs (A). DNA sequence of the *Mgat1b* fragment with the Bcl2 site highlighted and underlined (B). The forward and reverse gRNA pair used with CRISPR-Cas9 to mutate the *Mgat1b* gene (C).

Once microinjected embryos, developed to adults, DNA from tail clips of each adult was harvested and then amplified through Polymerase Chain Reaction (PCR). The amplified DNA was then digested with BclI and ran on an agarose gel to determine the number and sizes of the DNA fragments (Figure 14). The first lane contains an uncut wildtype DNA fragment used as a control. Lanes containing two DNA fragments indicate that the DNA was unaltered. Lanes containing one or three fragments show a resistance to BclI activity and indicate that one of the *Mgat1b* genes was mutated. Suspected *Mgat1b* mutant DNA was sent to identify sequence of indels. Two of the mutant fish selected were termed #10 and termed #21, named after a number assigned to them. The #10 mutant fish had a deletion of -AGA/TT and the #21 mutant fish had a mutation of -C/AGA/T.

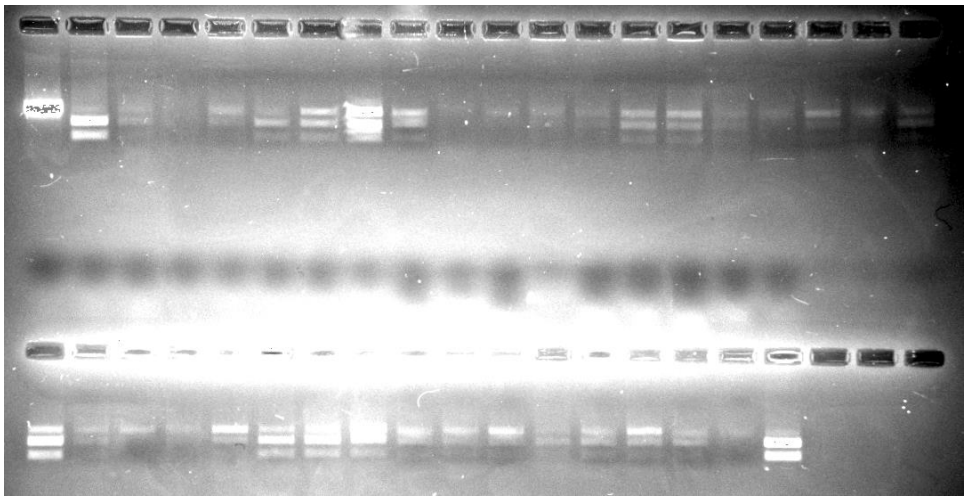

Figure 14. Successful knockout of *Mgat1b*. Injection of zebrafish embryos with gRNA plasmid grown to adulthood generating the F_0 generation. The first lane contains an uncut wildtype DNA fragment used as a control.

In order to generate an F_1 generation, the #10 mutant male fish with the mutation -AGA/TT was crossed with a wildtype female. Fin clippings of their offspring were collected and used for DNA isolation. The DNA was then amplified through PCR and treated with the restriction enzyme BclI. The DNA fragments were then separated via gel electrophoresis. Lanes with two bands indicate no resistance to BclI and are wild type fish. Lanes with three bands indicates that one copy of the *Mgat1b* gene has resistance to BclI and is therefore a heterozygous mutant fish. The upper band from numerous fish were sequenced to identify a male and a female with the -AGA/TT mutation. Both the 32♂ and 34♀ had the correct indel. They were used to generate the F_2 generation.

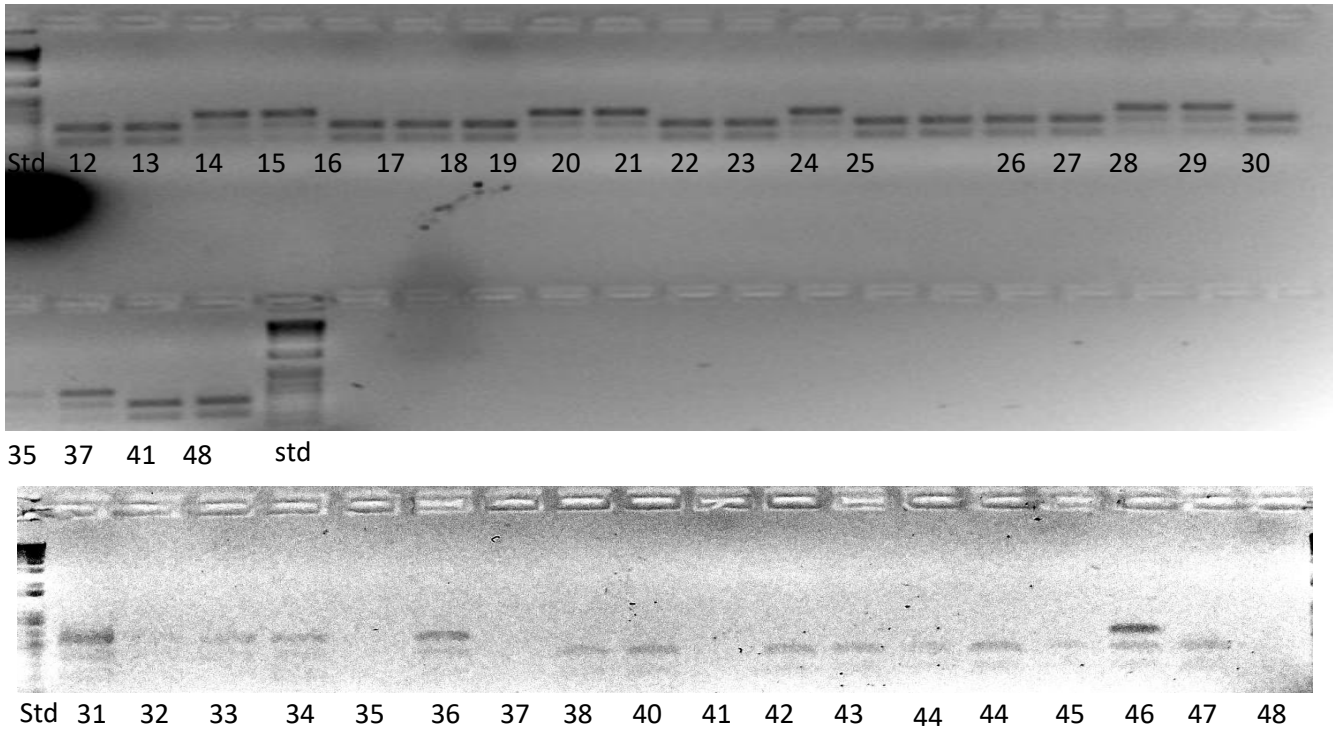

Figure 15. Generation of F_1 population from the #10 fish strain and showcase of fecundity. F_1: Mutant 10 male (-aga/tt) X WT female. Two bands indicate a wild type fish and three bands indicate a heterozygous mutant fish. The standard 1 KB was used to indicate the relative sizes of the DNA fragments.

In order to generate an F_2 population containing homozygous *Mgat1b* knockout fish, a male (32♂) and a female (34♀) of the F_1 generation with identical mutations were crossed. Fin clippings of their offspring were collected and used for DNA isolation. The DNA was then amplified through PCR and treated with the restriction enzyme BclI. The DNA fragments were then separated via gel electrophoresis. Lanes with two bands indicate no resistance to BclI and are wild type fish (+/+). Lanes with three bands indicates that one copy of the *Mgat1b* gene has resistance to BclI while the other was sensitive, and are therefore a heterozygous mutant fish (+/-). Lanes containing one band at 576bp indicate both copies of the *Mgat1b* gene are resistant to BclI and are therefore homozygous mutant fish (-/-). We then pooled the (+/+), (+/-), and (-/-) fish for future studies.

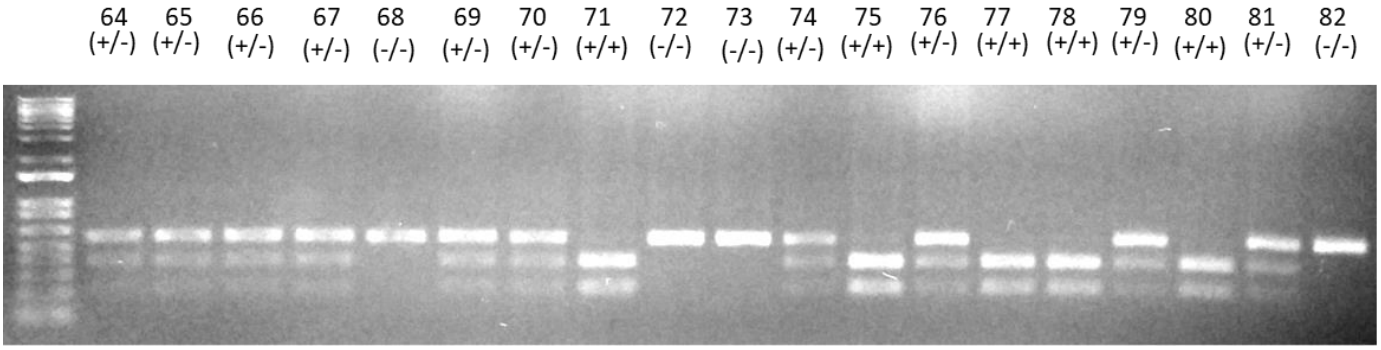

Figure 16. F_2 generation of the #10 fish strain. A heterozygous male and a heterozygous female from the F_1 population were crossed to generate the F_2 population. DNA of F_2 generation were separated via gel electrophoresis. Two bands indicated a wild type fish (+/+), three bands indicate a heterozygous mutant fish (+/-), and one band indicates a homozygous mutant fish (-/-).

To study the effect a increase in oligomannose type N-glycans have on embryo development, crosses between wild type fish (+/+), heterozygous mutant fish (+/-), and homozygous mutant fish (-/-) were conducted. Crosses of (+/+) with (+/+), (+/-) with (+/-), and (-/-) with (-/-) were performed during the early morning, when the lights in the fish facility first turn on. The number of viable embryos were determined at 0, 4, 8, 12, 18, and 24 hours post fertilization. The line graph shown in Figure 17A, represents the average percent of viable embryos over time. The wild type and heterozygous mutant crosses hardly show a decrease in embryo viability, with neither dropping below 92%. However, the mutant cross shows a significant decrease in embryo viability as compared to the heterozygous and wild type crosses at the 12, 18, and 24 hour time points. It is also important to note that the largest drop in embryo viability, for all crosses, happened between 8 and 12 hours past fertilization. The bar graph shown in Figure 17B represents the average percent viability at 24 hours post fertilization. We see a significant difference when comparing the embryo viability of the knockout (~70%) to that of the heterozygous (92%) and the wild type (98%). The average number of viable embryos spawned was also determined and shown in Figure 17C. The wild type crosses produced the fewest amount of embryos, the heterozygous crosses produced the most embryos, and the homozygous mutant crosses produced embryos in an amount between the other two. A significant difference was found between the heterozygous and wild type crosses. These results indicate that the loss of *Mgat1b* contributes to a decrease in survivor rate of embryos, and an increase in the number of embryo spawned.

A.

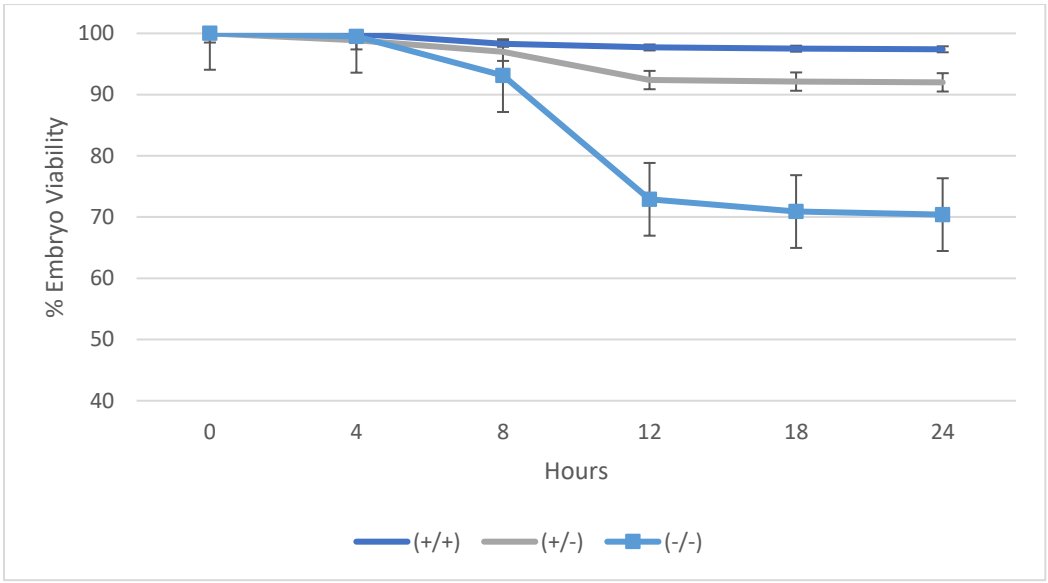
100
90
80
70
60
50
40
% Embryo Viability
0
4
8
12
18
24
Hours
(+/+)
(+/-)
(-/-)

B.

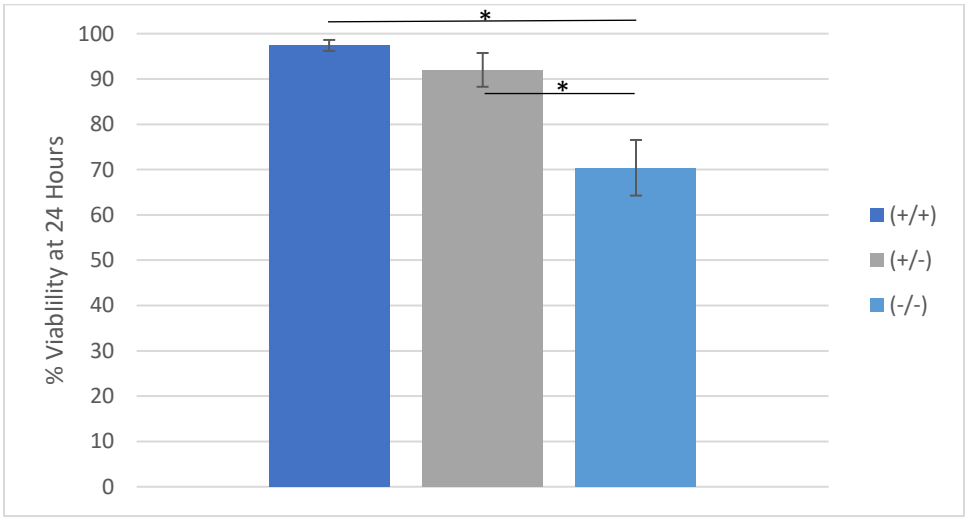
100
90
80
70
60
50
40
30
20
10
0
% Viablility at 24 Hours
*
*
(+/+)
(+/-)
(-/-)

C.

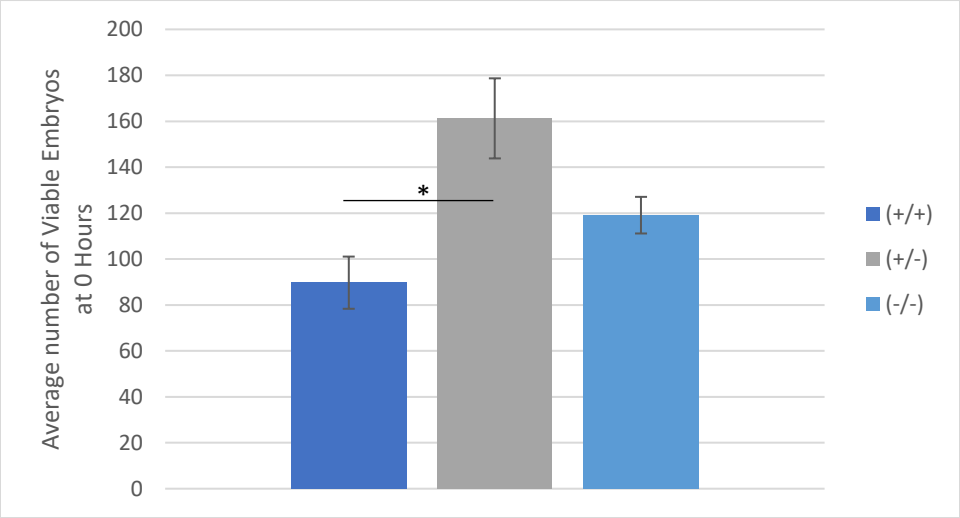

Figure 17. Zebrafish embryo viability decreases due to the increase of oligomannose type N-glycans. Crosses of (+/+) with (+/+), (+/-) with (+/-), and (-/-) with (-/-) were performed during the early morning. The number of viable embryos were determined at 0, 4, 8, 12, 18, and 24 hours post fertilization. The line graph represents the average percent of viable embryos over time (17A). The bar graph represents the average percent viability at 24 hours post fertilization (17B). The average number of viable embryos spawned was also determined (17C). Crosses were repeated n times where n=10 (+/+), n=8 (+/-), and n=10 (-/-). * indicates a significant difference at a $p<0.05$.

Discussion

In vitro, complex type N-glycans were substituted for hybrid type N-glycans in human and rat neuroblastoma (Hall et al. 2017) cell lines in order to determine how it affected aberrant neuronal properties. This was investigated through the silencing of the *Mgat2* gene using CRISPR-Cas9 technology. *Mgat2* encodes for the enzyme GlcNAcT-II, responsible for the conversion of hybrid type N-glycans to complex type N-Glycans (Stanley et al. 2017). Lectin binding studies were conducted to support that the HuNB(-*Mgat2*) cell line predominately expresses hybrid type N-glycans while the HuNB cell line expresses predominately complex type N-glycans. HuNB(-*Mgat2*) cells were transiently transfected with *Mgat2* to further support that the loss of complex type N-glycans are attributed to the loss of GlcNAcT-II, further indicating that any differences among cell lines is due to expression of different N-glycans. This provides a neuronal cell model that predominately expresses hybrid type N-glycans. Previously we engineered a rat neuroblastoma cell line predominately expressing hybrid type N-glycans (Hall et al. 2017; Hall et al. 2018). Here the goal is to establish an additional neuroblastoma cell line which has similar aberrant neuronal properties. The use of these cell lines will strongly support the role of complex type N-glycans in development and progression of neuroblastoma. Analysis of the cell line revealed that decreased amounts of complex type N-glycans with an increased amount of hybrid type N-glycans resulted in suppressed colony formation, MMP-2 expression and activity, and increased cell migration. Similar findings were observed for the rat *Mgat2* knockout cell line (Hall et al. 2017), indicating that complex N-glycans enhance tumorigenicity in neuroblastoma.

Kv3.1b, a voltage-gated potassium channel, was characterized to support an alteration in the N-glycosylation pathway through the silencing of *Mgat2.* Western blots supported that HuNB cells express Kv3.1b with complex type N-glycans while the HuNB(-*Mgat2*) cells express Kv3.1b with hybrid type N-glycans. Further, complex type N-glycans attached to Kv3.1b was also observed in various brain segments (Hall et al. 2015; Hall et al. 2016). In this previous study, we revealed that hybrid type N-glycans modified the distribution of the Kv3.1b protein between outgrowths and cell body, as well as, decreasing the opening and closing rates when compared to Kv3.1b with complex type N-glycans (Hall et al. 2017; Hall et al. 2018). In earlier studies, it was found that the number of N-glycans associated with Kv3.1b modified channel opening and closing rates, cell-cell adhesion, and cell migration (Hall et al 2011). Taken together, the N-glycosylation processing of Kv3.1b is critical for regulation the distribution of the Kv3.1b channels to the cell body and outgrowths, and the changes in N-glycan structure will result in changes in neuronal cellular properties.

The glycosylation of proteins is crucial in the realms of biochemistry because most of membrane proteins are N-glycosylated (Hall et al. 2013; Hall et al. 2014). N-glycosylation is important in regulating protein activity and serve several vital roles contributing to protein folding, protein assembly, stability, and interactions (Varki and Lowe 2009; Helenius and Aebi 2004; Hall et al. 2013; Hall et al. 2015). While outside the cell, N-glycans are involved in cellular recognition events that can give rise to cancerous properties (Hall et al. 2016; Hall at al. 2018). These cancerous properties include: cell signaling, cell migration, cell invasion, cell proliferation, and cell-cell adhesion (Hall et al. 2016). Changes in N-glycan structure have potential significant

roles in tumor development and progression (Fuster and Esko 2005). Previous research has shown that a less aggressive neuroblastoma cell line was revealed to have increased amounts of hybrid type N-glycans (Hu et al 2015). Earlier studies have also shown that higher levels of β1,6-branched N-glycans enhance metastatic potential (Dennis et al 1987). Our current research aligns with these findings using two neuroblastoma cell models. In both human and rat (Hall et al. 2018) cell lines, we see that the predominate expression of hybrid and loss of complex type N-glycans creates less aggressive neuroblastomas.

Cancer cells interact with the ECM, neighboring cells, growth factors, and cytokines affiliated with the ECM (Kessenbrock, Plaks, and Werb 2010; Murphy 2008). A few indications of cancer progression include migration, invasion, metastasis, and angiogenesis. Essential molecules for the initiation of these processes are MMPs since their proteolytic activity degrades cell adhesion molecules and the ECM (Gialeli, Theocharis, & Karamanos 2011). MMPs degrade E-cadherin and integrin interactions allowing for cells to detach from the ECM and surrounding cells, increasing cellular migration and invasion (Murphy 2008). MMP-2 is known to degrade the ECM, promote cell proliferation, and upregulate angiogenesis (Decock et al. 2008). We observed that cells with predominately complex type N-glycans expressed more active MMP-2 than cells with predominately hybrid type N-glycans. Neuroblastoma cells expressing predominately hybrid type N-glycans may express less MMP-2 due to alterations in the glycosylation sites of MMP regulators. Extracellular matrix metalloproteinase inducer is a cell surface glycoprotein with attachment of oligomannose and complex type N-glycans. This surface protein directly stimulates MMP production and the loss of N-

glycans has been shown to decrease MMP production (Huang et al. 2013). The loss of complex type N-glycans may have caused decreased activity, leading to a lower expression of MMP-2. Another protein of interest, tissue inhibitor of metalloproteinases (TIMPs) are important regulators of MMPs (Murphy et al. 1991). Altered glycosylation of TIMP-1 and TIMP-3 have a direct effect on MMP-2 activity, interfering with their interactions. MMPs have also been shown to possess two highly conserved N-glycosylation sites that may be glycosylated (Boon et al. 2016). The loss of MMP-2 activity may be attributed to an alteration in the catalytic site due to the loss of *Mgat2.* Much remains to be discovered about glycosylation effects on MMP activity.

Cancer cells that lack the ability to invade or metastasize into neighboring tissue grow into benign tumors (National Cancer Institute 2007). The ability of cells to grow independent of attachment is connected to tumorigenic and metastatic potentials and is used as an indicator for the transformation of cancerous cells (Mori et al 2009). Non-cancerous cells, when detached from their extracellular surface, undergo a form of programmed cell death called anoikis (Frisch and Screaton 2001). Cancer cells can undergo a series of genetic and epigenetic changes that allows cells to grow in suspension independent of external and internal signals (Frisch, Schaller and Cieply 2013). Through anchorage-independent growth assays, it was determined that cells expressing predominately complex type N-glycans grew larger and more cell colonies than cells predominately expressing hybrid type N-glycans. The same trend was previously show in rat neuroblastoma cell lines (Hall et al. 2018). Thus, complex N-glycans enhanced cellular growth independent of cell anchorage in neuroblastoma.

Protein interactions and cell signaling play a role in cell migratory rates (Todeshini and Hakomori 2008; Hall et al. 2016; Hall et al. 2018). Cell migration is critical in the metastatic spread of cancer cells and the formation of metastasis. Migratory cancer cells can undergo molecular and cellular changes by remodeling their cell-cell and cell-matrix adhesion (Yilmaz and Christofori 2010). Previous studies have shown that the reduction of N-glycans at the cell surface lessened the amount of E-cadherin at the cell-cell border, reducing the strength of cell-cell interactions (Hall et al. 2014). Wound healing assays were conducted to determine the role complex type N-glycans play in the migratory ability of a human neuroblastoma cell line. We observed that the substitution of complex type N-glycans for hybrid type N-glycans slightly increases cell migration. This increase in cell migration was also found in rat neuroblastoma (Hall et al. 2018) as well as a Chinese hamster ovary cell line (Hall et al. 2016). While a slight increase in migration was observed, we also found that cell invasion was markedly decreased (Hall et al. 2018).

To study the effects the increase of oligomannose type N-glycans have on growth and development, a zebrafish model with *Mgat1b* silenced was generated. *Mgat1b* encodes for GlcNAcT-I, responsible for the conversion of oligomannose type N-glycans to hybrid type, which is needed for production of complex type N-glycans (Stanley et al. 2009). Mutant fish strains, in theory, should express less GlcNAcT-I due to the partial loss or total loss of *Mgat1b*. But zebrafish possess a *Mgat1a* gene which also encodes for GlcNAcT-I (Erickson et al. 2017), which may compensate for the loss of *Mgat1b.* However, current studies in our lab support raised levels of oligomannose in heterozygous and knockout fish. Alterations in the process of N-glycosylation can lead

to congenital disorders of glycosylation (Jaeken 2010). The majority of CDG patients have a neurological disease affecting multiple systems, such as the central nervous system, cellular transport, muscle function, immunity, hormones, coagulation, and regulatory processes. The number of CDGs caused by N-glycosylation defects are still on the rise (Scott et al. 2014). Previous mouse studies, knocking out *Mgat1* has resulted in embryonic death due to defects in neural tube formation death (Ioffe and Stanley 1994), emphasizing the importance of the N-glycosylation pathway in multicellular organisms. As such, these fish strains will assist with evaluating neurogenesis in vertebrae.

Crosses of wild type with wild type, heterozygous with heterozygous, and homozygous mutant with homozygous mutant were performed. The number of viable embryos were determined at 0, 4, 8, 12, 18, and 24 hours past fertilization. A significant decrease in embryo viability between the homozygous mutant crosses and the other crosses were observed after 8 hours past fertilization. This decrease in viability is happening at the time of neural induction (Kimmel et al. 1995). During this process, numerous signaling factors promotes the cells in the dorsal ectoderm to form the neural plate, ~10 hours past fertilization. The neural plate then folds to form the neural keel, ~13 hours past fertilization, which then fuses into the neural rod ~16 hours past fertilization (Kimmel et al. 1995). We suspect that diminishing the levels of hybrid and complex type N-glycans may play a role in neural induction within zebrafish, since the greatest drop in viability was measured at 12 hours past fertilization. Therefore, these fish strains will help address the role of increased oligomannose type N-glycans in neurogenesis.

Decreased hybrid and complex type N-glycans may affect other processes involved in embryo development as N-glycans are known to influence cell signaling and various protein interactions (Varki and Lowe 2009; Helenius and Aebi 2004). Many factors affect egg production and spawning. Fish size, age, health, spawning time, spawning frequency, and the presence of male fish all affect egg production (Nasiadka and Clark 2012). Heterozygous mutant fish spawned the most eggs, followed by the homozygous mutant, and then wild type fish spawned the fewest. Our findings suggest that the partial loss of hybrid and complex type N-glycans must contribute to the increased production of zebrafish eggs.

We conclude N-glycans play a critical role in neuroblastoma tumorigenicity, and also the growth and development of vertebrae. The substitution of complex type N-glycans for hybrid type lessened neuroblastoma tumorigenicity by diminishing cell proliferation independent of anchorage and MMP-2 expression and activity. It is also proposed that the increase of oligomannose type N-glycans play a role in the development and viability of embryos in a zebrafish model by altering neural induction processes.

Future Studies

Regarding neuroblastoma cell studies, future studies will involve further generation of various N-glycosylation mutants and the analysis of cell invasiveness and other cancerous properties to identify how N-glycans alter progression of neuroblastoma. Cell cycle analysis of the HuNB and HuNB(-*Mgat2*) cells will be conducted to investigate how the substitution of complex type N-glycans for hybrid type affect cell cycle progression. Patch clamp studies should also be conducted on Kv3.1b channels to determine how the expression of hybrid type N-glycans affect the firing rate of this potassium channel in comparison to channels with predominately complex type N-glycans.

To further improve zebrafish breeding studies, instead of setting up the previously mentioned crosses, crosses of each fish strain and sex should be crossed with wild type fish. This way any differences in the number of embryos and viability of embryos can be attributed to sex as well. Meaning we can investigate any potential changes to sperm and egg production as a result of diminished levels of hybrid and complex type N-glycans. We are currently profiling the glycans in the wild type, heterozygous, and knockout fish strains. Lectin blots will be conducted to show an increase in oligomannose N-glycans in brain and spinal cord of the heterozygous and knockout fish. We will also establish another N-glycosylation mutant in zebrafish, knocking out the *Mgat1a* gene, to study its affects on neurogenesis. This *Mgat1a* mutant will be crossed with a *Mgat1b* mutant to generate a full *Mgat1* knockout in a vertebrae model, which will be used to study neurogenesis.

References

"Cancer". *World Health Organization*. 12 September 2018.

"Defining Cancer". *National Cancer Institute*. 17 September 2007.

Adolf, B., Chapouton, P., Lam, C. S., Topp, S., Tannhäuser, B., Strähle, U., ... & Bally-Cuif, L. (2006). Conserved and acquired features of adult neurogenesis in the zebrafish telencephalon. *Developmental biology*, *295*(1), 278-293.

Anand P, Kunnumakkara AB, Sundaram C, Harikumar KB, Tharakan ST, Lai OS, Sung B, Aggarwal BB (2008). "Cancer is a preventable disease that requires major lifestyle changes". *Pharmaceutical Research*. 25 (9): 2097–116. doi:10.1007/s11095-008-9661-9.

Armstrong, R. A. (2013). What causes Alzheimer's disease?. *Folia Neuropathologica*, *51*(3), 169-188.

Barão, S., Moechars, D., Lichtenthaler, S. F., & De Strooper, B. (2016). BACE1 physiological functions may limit its use as therapeutic target for Alzheimer's disease. *Trends in neurosciences*, *39*(3), 158-169.

Baye, L. M., & Link, B. A. (2008). Nuclear migration during retinal development. *Brain research*, *1192*, 29-36.

Biedler, J. L., Roffler-Tarlov, S., Schachner, M., & Freedman, L. S. (1978). Multiple neurotransmitter synthesis by human neuroblastoma cell lines and clones. *Cancer research*, *38*(11 Part 1), 3751-3757.

Boon, L., Ugarte-Berzal, E., Vandooren, J., & Opdenakker, G. (2016). Glycosylation of matrix metalloproteases and tissue inhibitors: present state, challenges and opportunities. *Biochemical Journal*, *473*(11), 1471-1482.

Bray, F., Ferlay, J., Soerjomataram, I., Siegel, R. L., Torre, L. A., & Jemal, A. (2018). Global cancer statistics 2018: GLOBOCAN estimates of incidence and mortality worldwide for 36 cancers in 185 countries. *CA: a cancer journal for clinicians*, *68*(6), 394-424.

Brooks, N. L., Corey, M. J., & Schwalbe, R. A. (2006). Characterization of N-glycosylation consensus sequences in the Kv3. 1 channel. *The FEBS journal*, *273*(14), 3287-3300.

C. Haass, C. Kaether, G. Thinakaran, S. SisodiaTrafficking and proteolytic processing of APP Cold Spring Harb. Perspect. Med., 2 (2012), p. a006270

Cai, X. D., Golde, T. E., & Younkin, S. G. (1993). Release of excess amyloid beta protein from a mutant amyloid beta protein precursor. *Science*, *259*(5094), 514-516.

Cartwright, T. A., Corey, M. J., & Schwalbe, R. A. (2007). Complex oligosaccharides are N-linked to Kv3 voltage-gated K+ channels in rat brain. *Biochimica et Biophysica Acta (BBA)-General Subjects*, *1770*(4), 666-671.

Croce CM (January 2008). "Oncogenes and cancer". *The New England Journal of Medicine*. 358 (5): 502–11. doi:10.1056/NEJMra072367

Cummings, R.; Etzler, M. Antibodies and Lectins in Glycan Analysis. In *Essentials of Glycobiology*, 2nd ed.; Varki, A., Cummings, R., Esko, J., Freeze, H., Stanley, P., Eds.; Cold Spring Harbor Laboratory Press: Cold Spring Harbor, NY, USA, 2009; Chapter 45.

Dahm R (2006). "The Zebrafish Exposed". *American Scientist*. 94(5): 446–53.

Decock J, Hendrickx W, Vanleeuw U, Van Belle V, Van Huffel S, Christiaens MR, Ye S & Paridaens R (2008) Plasma MMP1 and MMP8 expression in breast cancer: protective role of MMP8 against lymph node metastasis. *BMC Cancer* 20, 8–77.

Dennis, J. W., Laferte, S., Waghorne, C., Breitman, M. L., & Kerbel, R. S. (1987). Beta 1-6 branching of Asn-linked oligosaccharides is directly associated with metastasis. *Science*, *236*(4801), 582-585.

Dong Z, Yang N, Yeo S-Y, Chitnis A, Guo S (2012). Intralineage directional Notch signaling regulates self-renewal and differentiation of asymmetrically dividing radial glia. Neuron. 74: 65-78. 10.1016/j.neuron.2012.01.031.

Dooley, K., & Zon, L. I. (2000). Zebrafish: a model system for the study of human disease. *Current opinion in genetics & development*, *10*(3), 252-256.

Erickson, T., Morgan, C. P., Olt, J., Hardy, K., Busch-Nentwich, E., Maeda, R., ... & Marcotti, W. (2017). Integration of Tmc1/2 into the mechanotransduction complex in zebrafish hair cells is regulated by Transmembrane O-methyltransferase (Tomt). *Elife*, *6*, e28474.

Frank, H. Y., Yarov-Yarovoy, V., Gutman, G. A., & Catterall, W. A. (2005). Overview of molecular relationships in the voltage-gated ion channel superfamily. *Pharmacological reviews*, *57*(4), 387-395.

Frisch, S. M., & Screaton, R. A. (2001). Anoikis mechanisms. *Current opinion in cell biology*, *13*(5), 555-562.

Frisch, S. M., Schaller, M., & Cieply, B. (2013). Mechanisms that link the oncogenic epithelial–mesenchymal transition to suppression of anoikis. *J Cell Sci*, *126*(1), 21-29.

Fuster, Mark M., and Jeffrey D. Esko. "The sweet and sour of cancer: glycans as novel therapeutic targets." *Nature Reviews Cancer* 5.7 (2005): 526-542.

Gersten O, Wimoth JR. (2002). The cancer transition in Japan since 1951. *Demogr Res. 7:271-306.*

Gialeli, C., Theocharis, A. D., & Karamanos, N. K. (2011). Roles of matrix metalloproteinases in cancer progression and their pharmacological targeting. *The FEBS journal*, *278*(1), 16-27.

Goss, P. E., Baptiste, J., Fernandes, B., Baker, M., & Dennis, J. W. (1994). A phase I study of swainsonine in patients with advanced malignancies. *Cancer research*, *54*(6), 1450-1457.

Gutman GA, Chandy KG, Grissmer S, Lazdunski M, McKinnon D, Pardo LA, Robertson GA, Rudy B, Sanguinetti MC, Stühmer W, Wang X (December 2005). "International Union of Pharmacology. LIII. Nomenclature and molecular relationships of voltage-gated potassium channels". *Pharmacological Reviews*. 57 (4): 473–508.

Hall, M. K., Cartwright, T. A., Fleming, C. M., & Schwalbe, R. A. (2011). Importance of glycosylation on function of a potassium channel in neuroblastoma cells. *PloS one*, *6*(4), e19317.

Hall, M. K., Weidner, D. A., Dayal, S., & Schwalbe, R. A. (2014). Cell surface N-glycans influence the level of functional E-cadherin at the cell–cell border. *FEBS Open Bio*, *4*(1), 892-897.

Hall, M. K., Weidner, D. A., Dayal, S., Pak, E., Murashov, A. K., & Schwalbe, R. A. (2017). Membrane Distribution and Activity of a Neuronal Voltage-Gated K+ Channel is Modified by Replacement of Complex Type N-Glycans with Hybrid Type. *Journal of glycobiology*, *6*(3).

Hall, M. K., Weidner, D. A., Edwards, M. A., & Schwalbe, R. A. (2015). Complex N-glycans influence the spatial arrangement of voltage gated potassium channels in membranes of neuronal-derived cells. *PloS one*, *10*(9), e0137138.

Hall, M. K., Weidner, D. A., ming Chen, J., Bernetski, C. J., & Schwalbe, R. A. (2013). Glycan structures contain information for the spatial arrangement of glycoproteins in the plasma membrane. *PLoS One*, *8*(9), e75013.

Hall, M. K., Weidner, D. A., Whitman, A. A., & Schwalbe, R. A. (2018). Lack of complex type N-glycans lessens aberrant neuronal properties. *PloS one*, *13*(6), e0199202.

Hall, M., Weidner, D., Zhu, Y., Dayal, S., Whitman, A., & Schwalbe, R. (2016). Predominant expression of hybrid N-glycans has distinct cellular roles relative to complex and oligomannose N-glycans. *International journal of molecular sciences*, *17*(6), 925.

Helenius, A., & Aebi, M. (2004). Roles of N-linked glycans in the endoplasmic reticulum. *Annual review of biochemistry*, *73*(1), 1019-1049.

Ho, W. L., Hsu, W. M., Huang, M. C., Kadomatsu, K., & Nakagawara, A. (2016). Protein glycosylation in cancers and its potential therapeutic applications in neuroblastoma. *Journal of hematology & oncology*, *9*(1), 100.

Howe, K., Clark, M. D., Torroja, C. F., Torrance, J., Berthelot, C., Muffato, M., ... & McLaren, S. (2013). The zebrafish reference genome sequence and its relationship to the human genome. *Nature*, *496*(7446), 498.

Hu, Y., Mayampurath, A., Khan, S., Cohen, J. K., Mechref, Y., & Volchenboum, S. L. (2015). N-linked glycan profiling in neuroblastoma cell lines. *Journal of proteome research*, *14*(5), 2074-2081.

Huang, W., Luo, W. J., Zhu, P., Tang, J., Yu, X. L., Cui, H. Y., ... & Chen, Z. N. (2013). Modulation of CD147-induced matrix metalloproteinase activity: role of CD147 N-glycosylation. *Biochemical Journal*, *449*(2), 437-448.

Ioffe, E., & Stanley, P. (1994). Mice lacking N-acetylglucosaminyltransferase I activity die at mid-gestation, revealing an essential role for complex or hybrid N-linked carbohydrates. *Proceedings of the National Academy of Sciences*, *91*(2), 728-732.

Jaeken, Jaak & van den Heuvel, Lambert. (2014). Congenital Disorders of Glycosylation. 10.1007/978-3-642-40337-8_30.

Jaeken J (2010) Congenital disorders of glycosylation. Ann N Y Acad Sci 1214: 190–198.

Jones R (October 2007). "Let sleeping zebrafish lie: a new model for sleep studies". *PLoS Biology*. 5 (10): e281.

Kaczmarek, L. K. (2006). Non-conducting functions of voltage-gated ion channels. *Nature Reviews Neuroscience*, *7*(10), 761.

Kessenbrock K, Plaks V & Werb Z (2010) Matrix metalloproteinases: regulators of the tumor microenviroment. *Cell* 141, 52–67.

Kimmel, C. B., Ballard, W. W., Kimmel, S. R., Ullmann, B., & Schilling, T. F. (1995). Stages of embryonic development of the zebrafish. *Developmental dynamics*, *203*(3), 253-310.

Kizil, C., Kaslin, J., Kroehne, V., & Brand, M. (2012). Adult neurogenesis and brain regeneration in zebrafish. *Developmental neurobiology*, *72*(3), 429-461.

Kizuka, Y., Kitazume, S., & Taniguchi, N. (2017). N-glycan and Alzheimer's disease. *Biochimica et Biophysica Acta (BBA)-General Subjects*, *1861*(10), 2447-2454.

Knudson AG (November 2001). "Two genetic hits (more or less) to cancer". *Nature Reviews. Cancer*. 1 (2): 157–62. doi:10.1038/35101031.

Koonin, E. V., Makarova, K. S., & Zhang, F. (2017). Diversity, classification and evolution of CRISPR-Cas systems. *Current opinion in microbiology*, *37*, 67-78.

Lander, E. S. (2016). The heroes of CRISPR. *Cell*, *164*(1-2), 18-28.

Lee, S. Y., Lee, A., Chen, J., & MacKinnon, R. (2005). Structure of the KvAP voltage-dependent K+ channel and its dependence on the lipid membrane. *Proceedings of the National Academy of Sciences*, *102*(43), 15441-15446.

Liwosz, A.; Lei, T.; Kukuruzinska, M.A. *N*-glycosylation affects the molecular organization and stability of E-cadherin junctions. *J. Biol. Chem.* 2006, *281*, 23138–23149.

Loechel F, Fox JW, Murphy G, Albrechtsen R & Wewer UM (2000) ADAM 12-S Cleaves IGFBP-3 and IGFBP-5 and Is Inhibited by TIMP-3. *Biochem Biophys Res Commun* 278, 511–515.

Maris, J. M. (2010). Recent advances in neuroblastoma. *New England Journal of Medicine*, *362*(23), 2202-2211.

Matharu, N., Rattanasopha, S., Tamura, S., Maliskova, L., Wang, Y., Bernard, A., ... & Ahituv, N. (2019). CRISPR-mediated activation of a promoter or enhancer rescues obesity caused by haploinsufficiency. *Science*, *363*(6424), eaau0629.

Meeker, N. D., Hutchinson, S. A., Ho, L., & Trede, N. S. (2007). Method for isolation of PCR-ready genomic DNA from zebrafish tissues. *Biotechniques*, *43*(5), 610-614.

Mohanraju, P., Makarova, K. S., Zetsche, B., Zhang, F., Koonin, E. V., & Van der Oost, J. (2016). Diverse evolutionary roots and mechanistic variations of the CRISPR-Cas systems. *Science*, *353*(6299), aad5147.

Mori, S., Chang, J. T., Andrechek, E. R., Matsumura, N., Baba, T., Yao, G., … Nevins, J. R. (2009). Anchorage-independent cell growth signature identifies tumors with metastatic potential. *Oncogene*, *28*(31), 2796–2805. doi:10.1038/onc.2009.139

Mougiakos, I., Bosma, E. F., de Vos, W. M., van Kranenburg, R., & van der Oost, J. (2016). Next generation prokaryotic engineering: the CRISPR-Cas toolkit. *Trends in biotechnology*, *34*(7), 575-587.

Murphy G (2008) The ADAMs: signalling scissors in the tumour microenvironment. *Nat Rev Cancer* 8, 932–941.

Murphy G., Houbrechts A., Cockett M.I., Williamson R.A., O'Shea M., Docherty A.J. The N-terminal domain of tissue inhibitor of metalloproteinases retains metalloproteinase inhibitory activity. Biochemistry. 1991;30:8097–8102. doi: 10.1021/bi00247a001.

Narasimhan S, Freed JC, Schachter H. The effect of a "bisecting" N-acetylglucosaminyl group on the binding of biantennary, complex oligosaccharides to concanavalin A, Phaseolus vulgaris erythroagglutinin (E-PHA), and Ricinus communis agglutinin (RCA-120) immobilized on agarose. Carbohydrate research. 1986;149(1):65–83. Epub 1986/06/01. pmid:3731182.

Nasiadka, A., & Clark, M. D. (2012). Zebrafish breeding in the laboratory environment. *ILAR journal*, *53*(2), 161-168.

Omran, A. R. (1971). The epidemiologic transition: a theory of the epidemiology of population change. The Milbank Memorial Fund Quarterly, 49, 509-538.

Orger, M. B., & de Polavieja, G. G. (2017). Zebrafish behavior: opportunities and challenges. *Annual review of neuroscience*, *40*, 125-147.

Otey, C. A., Boukhelifa, M., & Maness, P. (2003). B35 neuroblastoma cells: an easily transfected, cultured cell model of central nervous system neurons. *Methods Cell Biol*, *71*, 287-304.

Parichy, D. M., Elizondo, M. R., Mills, M. G., Gordon, T. N., & Engeszer, R. E. (2009). Normal table of postembryonic zebrafish development: staging by externally visible anatomy of the living fish. *Developmental dynamics*, *238*(12), 2975-3015.

Park, C., Clements, K. N., Issa, F. A., & Ahn, S. (2018). Effects of social experience on the habituation rate of zebrafish startle escape response: empirical and computational analyses. *Frontiers in Neural Circuits*, *12*, 7.

Pinho, S.S.; Figueiredo, J.; Cabral, J.; Carvalho, S.; Dourado, J.; Gärtner, F.; Mendonfa, A.M.; Isaji, T.; Gu, J.; Carneiro, F.; *et al.* E-cadherin and adherens-junctions stability in gastric carcinoma: Functional implications of glycosyltransferases involving *N*-glycan branching biosynthesis, *N*-acetylglucosaminyltransferases III and V. *Biochim. Biophys. Acta* 2013, *1830*, 2690–2700.

Ranjan A., Kalraiya R.D. Invasive potential of melanoma cells correlates with the expression of MT1-MMP and regulated by modulating its association with motility receptors via N-glycosylation on the receptors. Biomed. Res. Int. 2014;2014:804680. doi: 10.1155/2014/804680.

Rodriguez-Menchaca, A. A., Adney, S. K., Tang, Q. Y., Meng, X. Y., Rosenhouse-Dantsker, A., Cui, M., & Logothetis, D. E. (2012). PIP2 controls voltage-sensor movement and pore opening of Kv channels through the S4–S5 linker. *Proceedings of the National Academy of Sciences*, *109*(36), E2399-E2408.

Roy R, Yang J & Moses AM (2009) Matrix Metalloproteinases as novel biomarkers and potential therapeutic targets in human cancer. *J Clin Oncol* 27, 5287–5297.

Rudd P.M., Dwek R.A. Glycosylation: heterogeneity and the 3D structure of proteins. Crit. Rev. Biochem. Mol. Biol. 1997;32:1–100. doi: 10.3109/10409239709085144.

Rudy, B., & McBain, C. J. (2001). Kv3 channels: voltage-gated K+ channels designed for high-frequency repetitive firing. *Trends in neurosciences*, *24*(9), 517-526.

Sander, J. D., Maeder, M. L., Reyon, D., Voytas, D. F., Joung, J. K., & Dobbs, D. (2010). ZiFiT (Zinc Finger Targeter): an updated zinc finger engineering tool. *Nucleic acids research*, *38*(suppl_2), W462-W468.

Sander, J. D., Zaback, P., Joung, J. K., Voytas, D. F., & Dobbs, D. (2007). Zinc Finger Targeter (ZiFiT): an engineered zinc finger/target site design tool. *Nucleic acids research*, *35*(suppl_2), W599-W605.

Schedin-Weiss, S., Winblad, B., & Tjernberg, L. O. (2014). The role of protein glycosylation in Alzheimer disease. *The FEBS journal*, *281*(1), 46-62.

Schmidt, R., Strähle, U., & Scholpp, S. (2013). Neurogenesis in zebrafish–from embryo to adult. *Neural development*, *8*(1), 3.

Schwarz, F., & Aebi, M. (2011). Mechanisms and principles of N-linked protein glycosylation. *Current opinion in structural biology*, *21*(5), 576-582.

Scott, K., Gadomski, T., Kozicz, T., & Morava, E. (2014). Congenital disorders of glycosylation: new defects and still counting. *Journal of inherited metabolic disease*, *37*(4), 609-617.

Shaheen, P. E., Stadler, W., Elson, P., Knox, J., Winquist, E., & Bukowski, R. M. (2005). Phase II study of the efficacy and safety of oral GD0039 in patients with locally advanced or metastatic renal cell carcinoma. *Investigational new drugs*, *23*(6), 577-581.

Shi, G., & Trimmer, J. S. (1999). Differential asparagine-linked glycosylation of voltage-gated K+ channels in mammalian brain and in transfected cells. *The Journal of membrane biology*, *168*(3), 265-273.

Singleman, C., & Holtzman, N. G. (2014). Growth and maturation in the zebrafish, Danio rerio: a staging tool for teaching and research. *Zebrafish*, *11*(4), 396-406.

“SK-N-BE(2)-C: Human Neuroblastoma Cell Line (ATCC CRL-2268).” *Memorial Sloan Kettering Cancer Center*, MSK Cancer Center, 2019, www.mskcc.org/research-advantage/support/technology/tangible-material/sk-n-be-2-c-human-neuroblastoma-cell-line.

Stanley P, Schachter H, Taniguchi N (2009). N-Glycans In: Varki A, Cummings R, Esko J, Freeze H, Stanley P, Bertozzi C, Hart G, Etzler M (Eds), Essentials of Glycobiology, 2nd Edition, Cold Spring Harbor Laboratory Press, Cold Spring Harbor.

Stanley P, Taniguchi N, Aebi M. N-Glycans (2017). In: Varki A, Cummings RD, Esko JD, et al., editors. Essentials of Glycobiology [Internet]. 3rd edition. Cold Spring Harbor (NY): Cold Spring Harbor Laboratory Press; 2015-2017. Chapter 9. Available from: https://www.ncbi.nlm.nih.gov/books/NBK453020/doi: 10.1101/glycobiology.3e.009

Sutton C.W., O'Neill J.A., Cottrell J.S. (1994). Site-specific characterization of glycoprotein carbohydrates by exoglycosidase digestion and laser desorption mass spectrometry. Anal. Biochem;218:34–46. doi: 10.1006/abio.1994.1138.

Tiwari-Woodruff S, Beltran-Parrazal L, Charles A, Keck T, Vu T, et al. (2006) K+ channel KV3.1 associates with OSP/claudin-11 and regulates oligodendrocyte development. Am J Physiol Cell Physiol 291: C687–698.

Todeschini, A. R., & Hakomori, S. I. (2008). Functional role of glycosphingolipids and gangliosides in control of cell adhesion, motility, and growth, through glycosynaptic microdomains. *Biochimica et Biophysica Acta (BBA)-General Subjects*, *1780*(3), 421-433.

Tulsiani, D. R., & Touster, O. (1983). Swainsonine causes the production of hybrid glycoproteins by human skin fibroblasts and rat liver Golgi preparations. *Journal of Biological chemistry*, *258*(12), 7578-7585.

Van den Steen P.E., Proost P., Grillet B., Brand D.D., Kang A.H., Van Damme J., Opdenakker G. (2002). Cleavage of denatured natural collagen type II by neutrophil gelatinase B reveals enzyme specificity, post-translational modifications in the substrate, and the formation of remnant epitopes in rheumatoid arthritis. FASEB J.;16:379–389. doi: 10.1096/fj.01-0688com.

Varki A, Lowe J (2009) Biological Roles of Glycans. In: Varki A, Cummings R, Esko J, Freeze H, Stanley P, et al., Essentials of Glycobiology. 2nd ed. Cold Spring Harbor: Cold Spring Harbor Laboratory Press. Chapter 6.

Waters, Michael F., et al.(2006). "Mutations in voltage-gated potassium channel KCNC3 cause degenerative and developmental central nervous system phenotypes." *Nature genetics* 38.4: 447-451.

Yellen G (2002). “The voltage-gated potassium channels and their relatives”. *Nature.* 419 (6902): 35-42. Doi: 10.1038/nature00978.

Yilmaz, M., & Christofori, G. (2010). Mechanisms of motility in metastasizing cells. *Molecular cancer research*, *8*(5), 629-642.

Yoshimura, M., Ihara, Y., Matsuzawa, Y. and Taniguchi, N. (1996) Aberrant glycosylation of E-cadherin enhances cell-cell binding to suppress metastasis. J. Biol. Chem. 271, 13811-13815.

Yoshimura, M., Nishikawa, A., Ihara, Y., Taniguchi, S. and Taniguchi, N. (1995) Suppression of lung metastasis of B16 mouse melanoma by N-acetylglucosaminyltransferase III gene transfection. Proc. Natl. Acad. Sci. U.S.A. 92, 8754- 8758.

Appendix A: Animal Care and Use Letter of Approval

ECU

Animal Care and Use Committee
212 Ed Warren Life Sciences Building | East Carolina University | Greenville, NC 27834-4354
252-744-2436 office | **252-744-2355** fax

February 5, 2019

Ruth Schwalbe, Ph.D.
Department of Biochemistry
Brody 5E
East Carolina University

Dear Dr. Schwalbe:

Your Animal Use Protocol entitled, "Roles of N-Glycans and Potassium Channels in Zebrafish" (AUP #C065) was reviewed by this institution's Animal Care and Use Committee on February 5, 2019. The following action was taken by the Committee:

"Approved as submitted"

Please contact Aaron Hinkle at 744-2997 prior to hazard use

A copy is enclosed for your laboratory files. Please be reminded that all animal procedures must be conducted as described in the approved Animal Use Protocol. Modifications of these procedures cannot be performed without prior approval of the ACUC. The Animal Welfare Act and Public Health Service Guidelines require the ACUC to suspend activities not in accordance with approved procedures and report such activities to the responsible University Official (Vice Chancellor for Health Sciences or Vice Chancellor for Academic Affairs) and appropriate federal Agencies. **Please ensure that all personnel associated with this protocol have access to this approved copy of the AUP and are familiar with its contents.**

Sincerely yours,

Susan McRae, Ph.D.
Chair, Animal Care and Use Committee

SM/jd

Enclosure

Appendix B: Letter of Completed IACUC Training

ECU

Animal Care and Use Committee
212 Ed Warren Life Sciences Building | East Carolina University | Greenville, NC 27834-4354
252-744-2436 office | **252-744-2355** fax

MEMORANDUM

TO: Austin Whitman
Department of Biochemistry

FROM: Dorcas O'Rourke, D.V.M.
University Veterinarian

SUBJECT: Certificate of Training
Training Date –12/17/18

DATE: December 17, 2018

This letter is provided to certify that you have completed training in humane methods of animal experimentation, proper handling of selected species of research animals, and methods for reporting deficiencies in animal care and treatment. The training was provided in accordance with U.S. Department of Agriculture (9 CFR 2.32) regulations and the Public Health Service Policy.

This training included information on ECU animal care organizational structure, regulatory requirements, IACUC procedures, program for veterinary and animal care, occupational health and safety program, and methods for reporting concerns. Information on biology and care, proper restraint and procedures, and allergies and zoonoses were also provided.

We suggest that you retain this letter in your training file for future reference.

Appendix C: AUP Amendment Form Including Austin Whitman

administrative approval 12/17/18

East Carolina University Animal Use Protocol (AUP) Amendment Form
Latest Revision, March 2016

FOR IACUC USE ONLY
AUP # D185e
Date received: 12/6/18
Full Review and date: Designated Reviewer and date:
Approval date: 12/17/18
Pain Category: C
Amendments approved: 2
Minor Amendment: 2 admin
Significant Amendment: If so, number?

Please fill out completely and email to davenportp@ecu.edu or iacuc@ecu.edu

PROJECT INFORMATION: Please list AUP Number and Title
AUP#185e Studies of Hormones and Receptors in Zebrafish

Principal Investigator:
Yong Zhu

1. Please explain in simple, non-technical language, the purpose or rationale for the protocol amendment.
Add and remove associates from AUP

2. Will different people use the animals or are new personnel being added to the AUP? Will previously approved personnel be assuming new roles or responsibilities?
Yes 3/9/18
If so, list qualifications and training.
Add: Dr. Ruth Schwalbe (SCHWALBER@ecu.edu), Mary Kristen Hall (HALLMA@ecu.edu) 12/17/18
Cody Hatchett, Austin Alexander Whitman (whitmana13@students.ecu.edu)
3/30/17 12/17/18
Remove: Keslee Snuggs, Yasmene Odeh, Amanda Rogers, Zayer Thet, Paul Delmus Bridgers, Thomas Miller, Emma R Daughtrey, Jennifer Lesniak, Elizabeth L Ryan, Alexandria Ivana Warren, Jalen Malik Barnes, Christopher Shaqueal Barnes

3. Have protocol related hazards (transgenic animals, infectious, chemical or biologic agents) changed with this amendment? No
If so, please describe the hazard and the oversight committee associated with this hazard (see AUP form II.C.1). If any hazardous agents have changed since the original AUP, please fill out the attached Hazardous Agents Form (Appendix 1). Oversight committee approval is required before the amendment can be approved by IACUC.
Click here to enter text

4. Please indicate changes to the animals or animal numbers by addressing them in parts a, b, and/or c.
a. Will the strain or sex of the animals change? No